Fadda, F., Rossetti, Z.L., 1998. Chronic ethanol consumption: from neuroadaptation to neurodegeneration. Prog. Neurobiol. 56, 385–431.

Filliol, D., Ghozland, S., Chluba, J., Martin, M., Matthes, H.W., Simonin, F., Befort, K., Gaveriaux-Ruff, C., Dierich, A., Lemeur, M., Valverde, O., Maldonado, R., Kieffer, B.L., 2000. Mice deficient for delta- and mu-opioid receptors exhibit opposing alterations of emotional responses. Nat. Genet. 25, 195–200.

Fuchs, P.N., Roza, C., Sora, I., Uhl, G., Raja, S.N., 1999. Characterization of mechanical withdrawal responses and effects of mu-, delta- and kappa-opioid agonists in normal and mu-opioid receptor knockout mice. Brain Res. 821, 480–486.

Fukuda, K., Kato, S., Morikawa, H., Shoda, T., Mori, K., 1996. Functional coupling of the delta-, mu-, and kappa-opioid receptors to MAP-kinase and arachidonate release in Chinese hamster ovary cells. J. Neurochem. 67, 1309–1316.

Gordon, A.S., Yao, L., Wu, Z.L., Coe, I.R., Diamond, I., 1997. Ethanol alters the subcellular localization of delta- and epsilon-protein kinase C in NG108-15 cells. Mol. Pharmacol. 52, 554–559.

Harris, R.A., Mcquilkin, S.J., Paylor, R., Abeliovich, A., Tonegawa, S., Wehner, J.M., 1995. Mutant mice lacking the gamma isoform of protein kinase C show decreased behavioral actions of ethanol and altered function of gamma-aminobutyrate type A receptors. Proc. Natl. Acad. Sci. USA 92, 3658–3662.

Hatakeyama, S., Wakamori, M., Ino, M., Miyamoto, N., Takahashi, E., Yoshinaga, T., Sawada, K., Imoto, K., Tanaka, I., Yoshizawa, T., Nishizawa, Y., Mori, Y., Niidome, T., Shoji, S., 2001. Differential nociceptive responses in mice lacking the α_{1B} subunit of N-type Ca^{2+} channels. Neuroreport 12, 2423–2427.

Hendry, I.A., Kelleher, K.L., Bartlett, S.E., Leck, K.J., Reynolds, A.J., Heydon, K., Mellick, A., Megirian, D., Matthaei, K.I., 2000. Hypertolerance to morphine in $G_{z\alpha}$-deficient mice. Brain Res. 870, 10–19.

Herlitze, S., Garcia, D.E., Mackie, K., Hille, B., Scheuer, T., Catterall, W.A., 1996. Modulation of Ca^{2+} channels by G-protein beta gamma subunits. Nature 380, 258–262.

Hodge, C.W., Mehmert, K.K., Kelley, S.P., McMahon, T., Haywood, A., Olive, M.F., Wang, D., Sanchez-Perez, A.M., Messing, R.O., 1999. Supersensitivity to allosteric $GABA_A$ receptor modulators and alcohol in mice lacking PKCε. Nat. Neurosci. 2, 997–1002.

Huang, C.L., Feng, S., Hilgemann, D.W., 1998. Direct activation of inward rectifier potassium channels by PIP_2 and its stabilization by Gβγ. Nature 391, 803–806.

Ikeda, K., Kobayashi, T., Ichikawa, T., Usui, H., Kumanishi, T., 1995. Functional couplings of the δ- and the κ-opioid receptors with the G-protein-activated K^+ channel. Biochem. Biophys. Res. Commun. 208, 302–308.

Ikeda, K., Kobayashi, T., Kumanishi, T., Niki, H., Yano, R., 2000. Involvement of G-protein-activated inwardly rectifying K^+ (GIRK) channels in opioid-induced analgesia. Neurosci. Res. 38, 113–116.

Ikeda, K., Kobayashi, T., Ichikawa, T., Usui, H., Abe, S., Kumanishi, T., 1996. Comparison of the three mouse G-protein-activated K^+ (GIRK) channels and functional couplings of the opioid receptors with the GIRK1 channel. Ann. N.Y. Acad. Sci. 801, 95–109.

Ikeda, K., Watanabe, M., Ichikawa, T., Kobayashi, T., Yano, R., Kumanishi, T., 1998. Distribution of prepro-nociceptin/orphanin FQ mRNA and its receptor mRNA in developing and adult mouse central nervous systems. J. Comp. Neurol. 399, 139–151.

Ikeda, K., Ichikawa, T., Kobayashi, T., Kumanishi, T., Oike, S., Yano, R., 1999. Unique behavioural phenotypes of recombinant-inbred CXBK mice: partial deficiency of sensitivity to μ- and κ-agonists. Neurosci. Res. 34, 149–155.

Ikeda, K., Kobayashi, T., Ichikawa, T., Kumanishi, T., Niki, H., Yano, R., 2001. The untranslated region of μ-opioid receptor mRNA contributes to reduced opioid sensitivity in CXBK mice. J. Neurosci. 21, 1334–1339.

Ikeda, K., Kobayashi, K., Kobayashi, T., Ichikawa, T., Kumanishi, T., Kishida, H., Yano, R., Manabe, T., 1997. Functional coupling of the nociceptin/orphanin FQ receptor with the G-protein-activated K^+ (GIRK) channel. Brain Res. Mol. Brain Res. 45, 117–126.

Ikeda, S.R., 1996. Voltage-dependent modulation of N-type calcium channels by G-protein beta gamma subunits. Nature 380, 255–258.

Jeong, S.W., Ikeda, S.R., 1998. G protein α subunit Gαz couples neurotransmitter receptors to ion channels in sympathetic neurons. Neuron 21, 1201–1212.

Jiang, M., Gold, M.S., Boulay, G., Spicher, K., Peyton, M., Brabet, P., Srinivasan, Y., Rudolph, U., Ellison, G., Birnbaumer, L., 1998. Multiple neurological abnormalities in mice deficient in the G protein Go. Proc. Natl. Acad. Sci. USA 95, 3269–3274.

Jordan, B.A., Devi, L.A., 1999. G-protein-coupled receptor heterodimerization modulates receptor function. Nature 399, 697–700.

Karschin, C., Dissmann, E., Stuhmer, W., Karschin, A., 1996. IRK(11–3) and GIRK(1–4) inwardly rectifying K^+ channel mRNAs are differentially expressed in the adult rat brain. J. Neurosci. 16, 3559–3570.

Karschin, C., Schreibmayer, W., Dascal, N., Lester, H., Davidson, N., Karschin, A., 1994. Distribution and localization of a G protein-coupled inwardly rectifying K^+ channel in the rat. FEBS Lett. 348, 139–144.

Kieffer, B.L., 1995. Recent advances in molecular recognition and signal transduction of active peptides: receptors for opioid peptides. Cell Mol. Neurobiol. 15, 615–635.

Kieffer, B.L., Befort, K., Gaveriaux-Ruff, C., Hirth, C.G., 1992. The delta-opioid receptor: isolation of a cDNA by expression cloning and pharmacological characterization. Proc. Natl. Acad. Sci. USA 89, 12048–12052.

Kim, C., Jun, K., Lee, T., Kim, S.S., McEnery, M.W., Chin, H., Kim, H.L., Park, J.M., Kim, D.K., Jung, S.J., Kim, J., Shin, H.S., 2001. Altered nociceptive response in mice deficient in the α_{1B} subunit of the voltage-dependent calcium channel. Mol. Cell Neurosci. 18, 235–245.

Kitchen, I., Slowe, S.J., Matthes, H.W., Kieffer, B., 1997. Quantitative autoradiographic mapping of mu-, delta- and kappa-opioid receptors in knockout mice lacking the mu-opioid receptor gene. Brain Res. 778, 73–88.

Kobayashi, T., Ikeda, K., Ichikawa, T., Abe, S., Togashi, S., Kumanishi, T., 1995. Molecular cloning of a mouse G-protein-activated K+ channel (mGIRK1) and distinct distributions of three GIRK (GIRK1, 2 and 3) mRNAs in mouse brain. Biochem. Biophys. Res. Commun. 208, 1166–1173.

Kobayashi, T., Ikeda, K., Kojima, H., Niki, H., Yano, R., Yoshioka, T., Kumanishi, T., 1999. Ethanol opens G-protein-activated inwardly rectifying K^+ channels. Nat. Neurosci. 2, 1091–1097.

Konig, M., Zimmer, A.M., Steiner, H., Holmes, P.V., Crawley, J.N., Brownstein, M.J., Zimmer, A., 1996. Pain responses, anxiety and aggression in mice deficient in pre-proenkephalin. Nature 383, 535–538.

Krapivinsky, G., Gordon, E.A., Wickman, K., Velimirovic, B., Krapivinsky, L., Clapham, D.E., 1995. The G-protein-gated atrial K^+ channel I_{KACh} is a heteromultimer of two inwardly rectifying K^+-channel proteins. Nature 374, 135–141.

Krauss, S.W., Ghirnikar, R.B., Diamond, I., Gordon, A.S., 1993. Inhibition of adenosine uptake by ethanol is specific for one class of nucleoside transporters. Mol. Pharmacol. 44, 1021–1026.

Kubo, Y., Reuveny, E., Slesinger, P.A., Jan, Y.N., Jan, L.Y., 1993. Primary structure and functional expression of a rat G-protein-coupled muscarinic potassium channel. Nature 364, 802–806.

Law, P.Y., Wong, Y.H., Loh, H.H., 2000. Molecular mechanisms and regulation of opioid receptor signaling. Annu. Rev. Pharmacol. Toxicol. 40, 389–430.

Lee, J.W., Joshi, S., Chan, J.S., Wong, Y.H., 1998. Differential coupling of mu-, delta-, and kappa-opioid receptors to Gα16-

mediated stimulation of phospholipase C. J. Neurochem. 70, 2203–2211.

Leonoudakis, D., Gray, A.T., Winegar, B.D., Kindler, C.H., Harada, M., Taylor, D.M., Chavez, R.A., Forsayeth, J.R., Yost, C.S., 1998. An open rectifier potassium channel with two pore domains in tandem cloned from rat cerebellum. J. Neurosci. 18, 868–877.

Lesage, F., Guillemare, E., Fink, M., Duprat, F., Heurteaux, C., Fosset, M., Romey, G., Barhanin, J., Lazdunski, M., 1995. Molecular properties of neuronal G-protein-activated inwardly rectifying K^+ channels. J. Biol. Chem. 270, 28660–28667.

Lewohl, J.M., Wilson, W.R., Mayfield, R.D., Brozowski, S.J., Morrisett, R.A., Harris, R.A., 1999. G-protein-coupled inwardly rectifying potassium channels are targets of alcohol action. Nat. Neurosci. 2, 1084–1090.

Li, C., Peoples, R.W., Weight, F.F., 1994. Alcohol action on a neuronal membrane receptor: evidence for a direct interaction with the receptor protein. Proc. Natl. Acad. Sci. USA 91, 8200–8204.

Li, L.Y., Chang, K.J., 1996. The stimulatory effect of opioids on MAP-kinase in Chinese hamster ovary cells transfected to express mu-opioid receptors. Mol. Pharmacol. 50, 599–602.

Liao, Y.J., Jan, Y.N., Jan, L.Y., 1996. Heteromultimerization of G-protein-gated inwardly rectifying K^+ channel proteins GIRK1 and GIRK2 and their altered expression in weaver brain. J. Neurosci. 16, 7137–7150.

Linder, M.E., Gilman, A.G., 1992. G proteins. Sci. Am. 267 (56-61), 55–64.

Lovinger, D.M., 1999. 5-HT_3 receptors and the neural actions of alcohols: an increasingly exciting topic. Neurochem. Int. 35, 125–130.

Lovinger, D.M., White, G., 1991. Ethanol potentiation of 5-HT_3 receptor-mediated ion current in neuroblastoma cells and isolated adult mammalian neurons. Mol. Pharmacol. 40, 263–270.

Lovinger, D.M., White, G., Weight, F.F., 1989. Ethanol inhibits NMDA-activated ion current in hippocampal neurons. Science 243, 1721–1724.

Lyon, R.C., McComb, J.A., Schreurs, J., Goldstein, D.B., 1981. A relationship between alcohol intoxication and the disordering of brain membranes by a series of short-chain alcohols. J. Pharmacol. Exp. Ther. 218, 669–675.

Mansour, A., Fox, C.A., Akil, H., Watson, S.J., 1995. Opioid receptor mRNA expression in the rat CNS: anatomical and functional implications. Trends Neurosci. 18, 22–29.

Matthes, H.W., Smadja, C., Valverde, O., Vonesch, J.L., Foutz, A.S., Boudinot, E., Denavit-Saubie, M., Severini, C., Negri, L., Roques, B.P., Maldonado, R., Kieffer, B.L., 1998. Activity of the delta-opioid receptor is partially reduced, whereas activity of the kappa-receptor is maintained in mice lacking the mu-receptor. J. Neurosci. 18, 7285–7295.

Matthes, H.W., Maldonado, R., Simonin, F., Valverde, O., Slowe, S., Kitchen, I., Befort, K., Dierich, A., Le Meur, M., Dolle, P., Tzavara, E., Hanoune, J., Roques, B.P., Kieffer, B.L., 1996. Loss of morphine-induced analgesia, reward effect and withdrawal symptoms in mice lacking the mu-opioid receptor gene. Nature 383, 819–823.

McCreery, M.J., Hunt, W.A., 1978. Physico-chemical correlates of alcohol intoxication. Neuropharmacology 17, 451–461.

Meunier, J.C., Mollereau, C., Toll, L., Suaudeau, C., Moisand, C., Alvinerie, P., Butour, J.L., Guillemot, J.C., Ferrara, P., Monsarrat, B., Mazarguil, H., Vassart, G., Parmentier, M., Costentin, J., 1995. Isolation and structure of the endogenous agonist of opioid receptor-like ORL1 receptor. Nature 377, 532–535.

Mihic, S.J., 1999. Acute effects of ethanol on $GABA_A$ and glycine receptor function. Neurochem. Int. 35, 115–123.

Minami, M., Satoh, M., 1995. Molecular biology of the opioid receptors: structures, functions and distributions. Neurosci. Res. 23, 121–145.

Mitrovic, I., Yi, E., Margeta-Mitrovic, M., Stoffel, M., Basbaum, A.I., 2000. Contribution of GIRK2 channels to morphine and clonidine antinociception: a possible mediator of sex differences. Soc. Neurosci. Abst. 26, 2188.

Miyakawa, T., Yagi, T., Kitazawa, H., Yasuda, M., Kawai, N., Tsuboi, K., Niki, H., 1997. Fyn-kinase as a determinant of ethanol sensitivity: relation to NMDA-receptor function. Science 278, 698–701.

Mollereau, C., Parmentier, M., Mailleux, P., Butour, J.L., Moisand, C., Chalon, P., Caput, D., Vassart, G., Meunier, J.C., 1994. ORL1, a novel member of the opioid receptor family. Cloning, functional expression and localization. FEBS Lett. 341, 33–38.

Muth, J.N., Varadi, G., Schwartz, A., 2001. Use of transgenic mice to study voltage-dependent Ca^{2+} channels. Trends Pharmacol. Sci. 22, 526–532.

Nagy, L.E., Diamond, I., Casso, D.J., Franklin, C., Gordon, A.S., 1990. Ethanol increases extracellular adenosine by inhibiting adenosine uptake via the nucleoside transporter. J. Biol. Chem. 265, 1946–1951.

Narahashi, T., Aistrup, G.L., Marszalec, W., Nagata, K., 1999. Neuronal nicotinic acetylcholine receptors: a new target site of ethanol. Neurochem. Int. 35, 131–141.

Narita, M., Mizoguchi, H., Sora, I., Uhl, G.R., Tseng, L.F., 1999. Absence of G-protein activation by mu-opioid receptor agonists in the spinal cord of mu-opioid receptor knockout mice. Br. J. Pharmacol 126, 451–456.

Navarro, B., Kennedy, M.E., Velimirovic, B., Bhat, D., Peterson, A.S., Clapham, D.E., 1996. Non-selective and Gβγ-insensitive weaver K^+ channels. Science 272, 1950–1953.

Nestler, E.J., 2001. Molecular neurobiology of addiction. Am. J. Addict. 10, 201–217.

Nestler, E.J., Duman, R.S., 1999. G proteins. In: Siegel, G.J., Agranoff, B.W., Albers, R.W., Fisher, S.K., Uhler, M.D. (Eds.), Basic Neurochemistry, sixth ed.. Lippincott-Raven, Philadelphia, pp. 401–414.

North, R.A., 1989. Drug receptors and the inhibition of nerve cells. Br. J. Pharmacol. 98, 13–28.

Ozaki M., Hashikawa T., Ikeda K., Miyakawa Y., Ichikawa T., Ishihara Y., Kumanishi T., Yano R. Degeneration of pontine mossy fibers during cerebellar development in weaver mutant mice. Eur. J. Neurosci., in press.

Pan, Z.Z., Williams, J.T., Osborne, P.B., 1990. Opioid actions on single nucleus raphe magnus neurons from rat and guinea-pig in vitro. J. Physiol. 427, 519–532.

Patel, A.J., Honore, E., 2001. Properties and modulation of mammalian 2P domain K^+ channels. Trends Neurosci. 24, 339–346.

Patil, N., Cox, D.R., Bhat, D., Faham, M., Myers, R.M., Peterson, A.S., 1995. A potassium channel mutation in weaver mice implicates membrane excitability in granule cell differentiation. Nat. Genet. 11, 126–129.

Peoples, R.W., Li, C., Weight, F.F., 1996. Lipid vs protein theories of alcohol action in the nervous system. Annu. Rev. Pharmacol. Toxicol. 36, 185–201.

Pert, C.B., Snyder, S.H., 1973. Opiate receptor: demonstration in nervous tissue. Science 179, 1011–1014.

Reimann, F., Ashcroft, F.M., 1999. Inwardly rectifying potassium channels. Curr. Opin. Cell Biol. 11, 503–508.

Reinscheid, R.K., Nothacker, H.P., Bourson, A., Ardati, A., Henningsen, R.A., Bunzow, J.R., Grandy, D.K., Langen, H., Monsma, F.J., Jr., Civelli, O., 1995. Orphanin FQ: a neuropeptide that activates an opioidlike G protein-coupled receptor. Science 270, 792–794.

Reuveny, E., Slesinger, P.A., Inglese, J., Morales, J.M., Iniguez-Lluhi, J.A., Lefkowitz, R.J., Bourne, H.R., Jan, Y.N., Jan, L.Y., 1994. Activation of the cloned muscarinic potassium channel by G protein beta gamma subunits. Nature 370, 143–146.

Rubinstein, M., Mogil, J.S., Japon, M., Chan, E.C., Allen, R.G., Low, M.J., 1996. Absence of opioid stress-induced analgesia in mice lacking β-endorphin by site-directed mutagenesis. Proc. Natl. Acad. Sci. USA 93, 3995–4000.

Saegusa, H., Kurihara, T., Zong, S., Kazuno, A., Matsuda, Y., Nonaka, T., Han, W., Toriyama, H., Tanabe, T., 2001. Suppression of inflammatory and neuropathic pain symptoms in mice lacking the N-type Ca^{2+} channel. EMBO J. 20, 2349–2356.

Saegusa, H., Kurihara, T., Zong, S., Minowa, O., Kazuno, A., Han, W., Matsuda, Y., Yamanaka, H., Osanai, M., Noda, T., Tanabe, T., 2000. Altered pain responses in mice lacking α_{1E} subunit of the voltage-dependent Ca^{2+} channel. Proc. Natl. Acad. Sci. USA 97, 6132–6137.

Sharifi, N., Diehl, N., Yaswen, L., Brennan, M.B., Hochgeschwender, U., 2001. Generation of dynorphin knockout mice. Brain Res. Mol. Brain Res. 86, 70–75.

Signorini, S., Liao, Y.J., Duncan, S.A., Jan, L.Y., Stoffel, M., 1997. Normal cerebellar development but susceptibility to seizures in mice lacking G protein-coupled, inwardly rectifying K^+ channel GIRK2. Proc. Natl. Acad. Sci. USA 94, 923–927.

Simon, M.I., Strathmann, M.P., Gautam, N., 1991. Diversity of G proteins in signal transduction. Science 252, 802–808.

Simonin, F., Valverde, O., Smadja, C., Slowe, S., Kitchen, I., Dierich, A., Le Meur, M., Roques, B.P., Maldonado, R., Kieffer, B.L., 1998. Disruption of the κ-opioid receptor gene in mice enhances sensitivity to chemical visceral pain, impairs pharmacological actions of the selective κ-agonist U-50,488H and attenuates morphine withdrawal. EMBO J. 17, 886–897.

Slater, S.J., Cox, K.J., Lombardi, J.V., Ho, C., Kelly, M.B., Rubin, E., Stubbs, C.D., 1993. Inhibition of protein kinase C by alcohols and anaesthetics. Nature 364, 82–84.

Slesinger, P.A., Patil, N., Liao, Y.J., Jan, Y.N., Jan, L.Y., Cox, D.R., 1996. Functional effects of the mouse weaver mutation on G protein-gated inwardly rectifying K^+ channels. Neuron 16, 321–331.

Sora, I., Funada, M., Uhl, G.R., 1997a. The mu-opioid receptor is necessary for [D-Pen2,D-Pen5]enkephalin-induced analgesia. Eur. J. Pharmacol. 324, R1–2.

Sora, I., Li, X.F., Funada, M., Kinsey, S., Uhl, G.R., 1999. Visceral chemical nociception in mice lacking mu-opioid receptors: effects of morphine, SNC80 and U-50,488. Eur. J. Pharmacol. 366, R3–5.

Sora, I., Takahashi, N., Funada, M., Ujike, H., Revay, R.S., Donovan, D.M., Miner, L.L., Uhl, G.R., 1997b. Opiate receptor knockout mice define mu receptor roles in endogenous nociceptive responses and morphine-induced analgesia. Proc. Natl. Acad. Sci. USA 94, 1544–1549.

Tanaka, C., Nishizuka, Y., 1994. The protein kinase C family for neuronal signaling. Annu. Rev. Neurosci. 17, 551–567.

Tecott, L.H., Maricq, A.V., Julius, D., 1993. Nervous system distribution of the serotonin 5-HT_3 receptor mRNA. Proc. Natl. Acad. Sci. USA 90, 1430–1434.

Thiele, T.E., Willis, B., Stadler, J., Reynolds, J.G., Bernstein, I.L., McKnight, G.S., 2000. High ethanol consumption and low sensitivity to ethanol-induced sedation in protein kinase A-mutant mice. J. Neurosci. 20, RC75.

Ueda, H., Miyamae, T., Hayashi, C., Watanabe, S., Fukushima, N., Sasaki, Y., Iwamura, T., Misu, Y., 1995. Protein kinase C involvement in homologous desensitization of delta-opioid receptor coupled to Gil-phospholipase C activation in Xenopus oocytes. J. Neurosci. 15, 7485–7499.

Vaccarino, A.L., Kastin, A.J., 1999. Endogenous opiates. Peptides 21, 1975–2034.

Wall, P.D., Melzack, R., 1999. Textbook of Pain, fourth ed.. Churchill Livingstone, Edinburgh.

Walter, H.J., Messing, R.O., 1999. Regulation of neuronal voltage-gated calcium channels by ethanol. Neurochem. Int. 35, 95–101.

Wand, G., Levine, M., Zweifel, L., Schwindinger, W., Abel, T., 2001. The cAMP-protein kinase A signal transduction pathway modulates ethanol consumption and sedative effects of ethanol. J. Neurosci. 21, 5297–5303.

Weight, F.F., Li, C., Peoples, R.W., 1999. Alcohol action on membrane ion channels gated by extracellular ATP (P2X receptors). Neurochem. Int. 35, 143–152.

Weiner, J.L., Valenzuela, C.F., Watson, P.L., Frazier, C.J., Dunwiddie, T.V., 1997. Elevation of basal protein kinase C activity increases ethanol sensitivity of $GABA_A$ receptors in rat hippocampal CA1 pyramidal neurons. J. Neurochem. 68, 1949–1959.

Wickman, K., Nemec, J., Gendler, S.J., Clapham, D.E., 1998. Abnormal heart rate regulation in GIRK4 knockout mice. Neuron 20, 103–114.

Woodward, J.J., 1999. Ionotropic glutamate receptors as sites of action for ethanol in the brain. Neurochem. Int. 35, 107–113.

Woodward, J.J., 2000. Ethanol and NMDA receptor signaling. Crit. Rev. Neurobiol. 14, 69–89.

Xie, W., Samoriski, G.M., McLaughlin, J.P., Romoser, V.A., Smrcka, A., Hinkle, P.M., Bidlack, J.M., Gross, R.A., Jiang, H., Wu, D., 1999. Genetic alteration of phospholipase Cβ3 expression modulates behavioral and cellular responses to μ opioids. Proc. Natl. Acad. Sci. USA 96, 10385–10390.

Xiong, K., Li, C., Weight, F.F., 2000. Inhibition by ethanol of rat P2X(4) receptors expressed in Xenopus oocytes. Br. J. Pharmacol. 130, 1394–1398.

Zadina, J.E., Hackler, L., Ge, L.J., Kastin, A.J., 1997. A potent and selective endogenous agonist for the mu-opiate receptor. Nature 386, 499–502.

Zhang, H., He, C., Yan, X., Mirshahi, T., Logothetis, D.E., 1999. Activation of inwardly rectifying K^+ channels by distinct PtdIns(4,5)P2 interactions. Nat. Cell Biol. 1, 183–188.

Zhou, W., Arrabit, C., Choe, S., Slesinger, P.A., 2001. Mechanism underlying bupivacaine inhibition of G protein-gated inwardly rectifying K^+ channels. Proc. Natl. Acad. Sci. USA 98, 6482–6487.

Zhu, Y., King, M.A., Schuller, A.G., Nitsche, J.F., Reidl, M., Elde, R.P., Unterwald, E., Pasternak, G.W., Pintar, J.E., 1999. Retention of supraspinal delta-like analgesia and loss of morphine tolerance in δ opioid receptor knockout mice. Neuron 24, 243–252.

Zimmer, A., Valjent, E., Konig, M., Zimmer, A.M., Robledo, P., Hahn, H., Valverde, O., Maldonado, R., 2001. Absence of Δ-9-tetrahydrocannabinol dysphoric effects in dynorphin-deficient mice. J. Neurosci. 21, 9499–9505.

British Journal of Pharmacology (2002) 135, 313–322
www.nature.com/bjp

Functional characterization of an endogenous *Xenopus* oocyte adenosine receptor

*,[1]Toru Kobayashi, [2,3]Kazutaka Ikeda & [1,4]Toshiro Kumanishi

[1]Department of Molecular Neuropathology, Brain Research Institute, Niigata University, 1-757 Asahimachi, Niigata, Niigata 951-8585, Japan; [2]Department of Molecular Psychiatry, Tokyo Institute of Psychiatry, 2-1-8 Kamikitazawa, Setagaya-ku, Tokyo 156-8585, Japan; [3]Laboratory for Neurobiology of Emotion, Brain Science Institute, RIKEN, 2-1 Hirosawa, Wako, Saitama 351-0198, Japan and [4]Niigata Longevity Research Institute, 766 Shimoishikawa, Shibata, Niigata 959-2516, Japan

1 To investigate the effects of adenosine on endogenous *Xenopus* oocyte receptors, we analysed defolliculated oocytes injected with mRNAs for the G protein-activated inwardly rectifying K^+ (GIRK) channels.

2 In oocytes injected with mRNAs for either GIRK1/GIRK2 or GIRK1/GIRK4 subunits, application of adenosine or ATP reversibly induced inward K^+ currents, although ATP was less potent than adenosine. The responses were attenuated by caffeine, a non-selective adenosine receptor antagonist. Furthermore, in uninjected oocytes from the same donor, adenosine produced no significant current.

3 The endogenous receptor was activated by two selective A_1 adenosine receptor agonists, N^6-cyclopentyladenosine (CPA) and N^6-cyclohexyladenosine (CHA), and antagonized by a selective A_1 adenosine receptor antagonist, 1,3-dipropyl-8-cyclopenylxanthine (DPCPX) at moderate nanomolar concentrations, but insensitive to micromolar concentrations of selective A_{2A} and A_3 adenosine receptor agonists, 2-[*p*-(2-carbonyl-ethyl)-phenylethylamino]-5′-N-ethylcarboxamidoadenosine (CGS21680) and N^6-(3-iodobenzyl)-5′-(N-methylcarbamoyl)adenosine (IB-MECA), respectively. However, the pharmacological characteristics of the receptor were different from those of the cloned *Xenopus* A_1 adenosine receptor and previously proposed adenosine receptors.

4 The adenosine-induced GIRK currents were abolished by injection of pertussis toxin and CPA inhibited forskolin-stimulated cyclic AMP accumulation.

5 We conclude that an adenosine receptor on the *Xenopus* oocyte membrane can activate GIRK channels and inhibit adenylyl cyclase *via* $G_{i/o}$ proteins. Moreover, our results suggest the existence of an endogenous adenosine receptor with the unique pharmacological characteristics. As the receptor was activated by nanomolar concentrations of adenosine, which is a normal constituent of extracellular fluid, the receptor may be involved in some effects through the $G_{i/o}$ protein signalling pathways in ovarian physiology.

British Journal of Pharmacology (2002) **135**, 313–322

Keywords: Adenosine receptor; $G_{i/o}$ protein; G protein-activated inwardly rectifying K^+ (GIRK) channel; *Xenopus* oocyte

Abbreviations: Ado, adenosine; CHA, N^6-cyclohexyladenosine; CGS21680, 2-[*p*-(2-carbonyl-ethyl)-phenylethylamino]-5′-N-ethylcarboxamidoadenosine; CPA, N^6-cyclopentyladenosine; DMSO, dimethyl sulphoxide; DPCPX, 1,3-dipropyl-8-cyclopenylxanthine; E_K, K^+ equilibrium potential; $G\beta\gamma$, G protein $\beta\gamma$-subunits; $G_{i/o}$, G_i and G_o; GIRK, G protein-activated inwardly rectifying K^+ channel; GPCR, G protein-coupled receptor; hK, high-potassium; IB-MECA, N^6-(3-iodobenzyl)-5′-(N-methylcarbamoyl)adenosine; ND98, K^+-free high-sodium; NECA, 5′-(*N*-ethylcarboxaminido)adenosine; n_H, Hill coefficient; PCR, polymerase chain reaction; PTX, pertussis toxin; XA_1, *Xenopus* A_1 adenosine receptor; XIR, endogenous *Xenopus* oocyte GIRK-related polypeptides

Introduction

Xenopus ovarian follicles consist of an oocyte surrounded by a vitelline envelope, follicle cells and thecal tissues (Fraser & Djamgoz, 1992). Mature follicular oocytes (stage V and VI) are known to possess receptors for adenosine and ATP as well as for acetylcholine, serotonin, dopamine, prostaglandins and progesterone (Dascal, 1987; Fraser & Djamgoz, 1992). The maturation phenomenon of *Xenopus* oocytes serves as a useful experimental model for studying its complicated mechanism, and is affected by adenosine (Gelerstein *et al.*, 1988). Oocytes of *Xenopus laevis* are also used widely in studies of mammalian neurotransmitter/hormone receptors and ion channels, which can be expressed in the oocyte membrane by microinjection of foreign RNAs. Examining receptor systems and channels in naive oocytes is therefore important in terms of ovarian physiology and for interpreting the functions of foreign receptors and channels when expressed in oocytes.

Adenosine is a normal constituent of intra- and extracellular fluids (Fredholm, 1995). Adenosine is released from cells that are metabolically active or stressed, and modulates the activity of various cells via the adenosine receptors (Collis & Hourani, 1993; Fredholm, 1995). To date, four adenosine receptor subtypes, A_1, A_{2A}, A_{2B} and A_3, have been identified

*Author for correspondence at: Department of Molecular Neuropathology, Brain Research Institute, Niigata University, 1-757 Asahimachi, Niigata, Niigata 951-8585, Japan;
E-mail: torukoba@bri.niigata-u.ac.jp

and pharmacologically characterized (Collis & Hourani, 1993; Poulsen & Quinn, 1998; Ralevic & Burnstock, 1998). All of these subtypes belong to the superfamily of G protein-coupled receptors (GPCRs), with the A_1 and A_3 adenosine receptors interacting with pertussis toxin (PTX)-sensitive G proteins, including G_i and G_o ($G_{i/o}$) proteins, and the A_{2A} and A_{2B} adenosine receptors interacting with G_s protein. Also, the A_{2B} and A_3 adenosine receptors are coupled to G_q protein. Furthermore, physiological, pharmacological and biochemical studies have suggested the existence of additional adenosine receptors that have not yet been identified. In follicular oocytes of *Xenopus laevis*, adenosine activated adenylyl cyclase and elicited cyclic AMP-mediated outward K^+ currents (Lotan *et al.*, 1982; 1985) but the effects were either abolished or markedly reduced by defolliculation, indicating that the receptors for adenosine are located in the follicle cells (Miledi & Woodward, 1989; Greenfield *et al.*, 1990a,b; King *et al.*, 1996). However, Gelerstein *et al.* (1988) showed that adenosine elevated cyclic AMP levels in defolliculated oocytes to the same extent as in follicular oocytes, suggesting that an adenosine receptor is also located on the oocyte membrane. In contrast, adenosine at high micromolar concentrations inhibited adenylyl cyclase activity in the defolliculated oocyte membrane fraction (Finidori *et al.*, 1982). In addition, previous studies using a variety of mammalian tissue preparations have suggested the existence of putatively additional subtypes of adenosine receptors (Shinozuka *et al.*, 1988; Daut *et al.*, 1990; Kirsch *et al.*, 1990; Forsyth *et al.*, 1991; Cornfield *et al.*, 1992; Abebe *et al.*, 1994). These findings suggest the possibility that there are additional endogenous adenosine receptors on the oocyte membrane. Although extensive studies using molecular biological techniques have elucidated the functional roles of the adenosine receptor subtypes (Nyce, 1999), the molecular and cellular mechanisms of action of the adenosine receptors in *Xenopus* oocytes remain poorly understood.

Various GPCRs, such as M_2 muscarinic, α_2 adrenergic, D_2 dopamine, opioid, nociceptin/orphanin FQ receptors and A_1 adenosine receptor, functionally couple to G protein-activated inwardly rectifying K^+ (GIRK) channels *via* interaction with $G_{i/o}$ proteins (North, 1989; Brown & Birnbaumer, 1990; Ikeda *et al.*, 1995; 1996; 1997; Pfaff & Karschin, 1997). Taken together with inhibition of adenylyl cyclase by adenosine in the oocyte membrane (Finidori *et al.*, 1982), unknown oocyte receptors for adenosine may also be able to activate GIRK channels as a signalling pathway. Hence, we examined the responses of endogenous *Xenopus* oocyte receptors to adenosine in defolliculated oocytes expressing GIRK channels. Here we demonstrate that an endogenous adenosine receptor on the *Xenopus* oocyte membrane can activate GIRK channels *via* $G_{i/o}$ proteins and inhibit forskolin-stimulated cyclic AMP accumulation and that the receptor shows unique pharmacological characteristics for adenosine receptor ligands.

Methods

Molecular biology

Plasmids containing the entire coding sequences for mouse GIRK1, GIRK2 and GIRK4 channel subunits were obtained using the polymerase chain reaction (PCR) method as described previously (Kobayashi *et al.*, 1995; 2000). Based on the cDNA sequence for the *Xenopus* A_1 adenosine (XA_1) receptor (GenBank/EMBL/DDBJ databases: accession number AJ249842), a pair of oligonucleotide primers corresponding to the regions containing either a translational initiation codon or a stop codon were synthesized. Primers for the XA_1 receptor were 5′-GCCCATGGGAATCCCAGCCTCGCTTGCT-3′ and 5′-GCTCTAGAGGACATTTTTAGAACTCTCAC-3′. The template cDNA was synthesized using mRNA prepared from *Xenopus laevis* oocytes and surrounding tissues and the 1st-Strand cDNA Synthesis Kit (Clontech) as described previously (Ikeda *et al.*, 2001). PCR was carried out using *Pfu* DNA polymerase (Stratagene) as described previously (Ikeda *et al.*, 1995). The PCR product was inserted into the plasmid pSP35T to yield the plasmid pSPXA1 and the cDNA insert was sequenced using an automated DNA sequencer model 373S (Applied Biosystems Inc.). The specific mRNAs were synthesized *in vitro* from the linearized plasmids using the mMESSAGE mMACHINE™ *In Vitro* Transcription Kit (Ambion).

Electrophysiological analyses

Adult female *Xenopus laevis* frogs were purchased from Copacetic (Soma, Aomori, Japan) and maintained in the laboratory until use. Frogs were anaesthetized by immersion in water including 0.15% tricaine (Sigma Chemical Co.). A small incision was made on the abdomen to remove several ovarian lobes from the frogs that were humanely killed after the final collection. Oocytes (Stage V and VI) were isolated manually from the ovary and maintained in Barth's solution (composition in mM: NaCl 88, KCl 1, $Ca(NO_3)_2$ 0.33, $CaCl_2$ 0.41, $MgSO_4$ 0.82, $NaHCO_3$ 2.4, Tris-HCl 7.5 (pH 7.4), and 0.1 mg ml^{-1} gentamicin sulphate; Wako Pure Chemical Industries). Oocytes were injected with either GIRK1 and GIRK2 mRNAs or GIRK1 and GIRK4 mRNAs (~0.6 ng of each mRNA per oocyte) and/or XA_1 receptor mRNA (~10 ng per oocyte). The oocytes were incubated at 19°C in Barth's solution, and defolliculated by manual dissection after treatment with 0.8 mg ml^{-1} collagenase (Wako Pure Chemical Industries) for 1 h (Kobayashi *et al.*, 1998). Whole-cell currents of the oocytes were recorded at 18–19°C from 2 to 7 days after injection with a conventional two-electrode voltage clamp (Kobayashi *et al.*, 2000). The membrane potential was held at −70 mV, unless otherwise specified. Microelectrodes were filled with 3M KCl. The oocytes were placed in a 0.05 ml narrow chamber and superfused continuously with a high-potassium (hK) solution (composition in mM: KCl 96, NaCl 2, $MgCl_2$ 1 and $CaCl_2$ 1.5) or a K^+-free high-sodium (ND98) solution (composition in mM: NaCl 98, $MgCl_2$ 1 and $CaCl_2$ 1.5) at a flow rate of 2.5 ml min^{-1}. In the hK solution, the K^+ equilibrium potential (E_K) is close to 0 mV and enables K^+ inward current flow through inward-rectifier K^+ channels at negative holding potentials. Agonist effect was expressed as a ratio of maximal effect induced by adenosine. Antagonist effect was quantified by dividing amplitude of adenosine-induced current in the presence of an antagonist by amplitude of adenosine-induced current without the antagonist. Data were fitted to a standard logistic equation using SigmaPlot (Jandel Scientific) to compute the EC_{50}, the IC_{50} and the Hill

coefficient (n_H) in analysis of concentration-response relationships.

Pertussis toxin treatment

For PTX (Sigma Chemical Co.) experiments (Kobayashi *et al.*, 1999), ~1.38 ng of PTX (0.1 $\mu g\ \mu l^{-1}$ in distilled water) per oocyte was injected 7 h before recording using a Nanoliter injector (World Precision Instruments). Oocytes of the control group were prepared from the same donor and sham injected with the same volume of distilled water.

Cyclic AMP assay

Cyclic AMP levels in *Xenopus* oocytes were determined using the Biotrak™ cAMP enzymeimmunoassay system (Amersham Pharmacia Biotech). Groups of 25 defolliculated oocytes carefully selected from the same donor on the basis of morphological similarity were incubated at room temperature for 30 min in Barth's solution containing N^6-cyclopentyladenosine (CPA) or forskolin (Wako Pure Chemical Industries). The incubation solution was replaced with a lysis reagent buffer containing 0.25% dodecyltrimethylammonium bromide in the kit, homogenized and centrifuged at $10,000 \times g$ for 10 min at 4°C. The measurements of cyclic AMP contents in the diluted supernatants were conducted according to the manufacture's procedure.

Statistical analysis of results

The values obtained are expressed as mean ± s.e.mean, and n is the number of oocytes tested. Statistical analysis of differences between groups was carried out using Student's t-test. A probability of 0.05 was taken as the level of statistical significance.

Compounds

All the compounds used were purchased from Research Biochemicals International. N^6-(3-iodobenzyl)-5'-(N-methylcarbamoyl)adenosine (IB-MECA) and 1,3-dipropyl-8-cyclopenylxanthine (DPCPX) were dissolved in dimethyl sulphoxide (DMSO). Other compounds were dissolved in distilled water. The stock solutions of all compounds were stored at −20°C until use. Each compound was added to the perfusion solution in appropriate amounts immediately before the experiments.

Results

Activation of GIRK channels by an endogenous adenosine receptor in Xenopus *oocytes*

Using the *Xenopus* oocyte system expressing GIRK channels (Kobayashi *et al.*, 1999), we investigated whether endogenous adenosine receptors in defolliculated oocytes activate GIRK channels. In oocytes injected with mRNAs for GIRK 1 and GIRK2 subunits, application of adenosine reversibly induced inward currents in a concentration-dependent manner in hK perfusion solution containing 96 mM K^+ and 2 mM Na^+ (Figure 1a, b). The EC_{50} and n_H values obtained from the concentration-response relationships were 917.3 ± 69.4 nM and 0.88 ± 0.02 (n = 10), respectively (Figure 1b and Table 1). The current responses to 3 μM adenosine were attenuated by caffeine, a non-selective adenosine receptor antagonist of methylxanthines, with the IC_{50} value of 245.5 ± 18.5 μM and n_H value of 0.72 ± 0.04 (n = 8) (Figures 1a and 2d). Although micromolar concentrations of ATP also induced inward currents, which were sensitive to caffeine, ATP was much less potent than adenosine (Figure 1b). These results suggest the existence of an endogenous receptor for adenosine in defolliculated oocytes. Moreover, the current responses to adenosine were completely abolished in the presence of 3 mM Ba^{2+}, a GIRK channel blocker (Dascal *et al.*, 1993), (n = 8, Figure 1a) which also blocked basally active GIRK currents (IC_{50} value of 170.7 ± 12.2 μM, n = 6; Kobayashi *et al.*, 2000). In contrast, in uninjected oocytes from the same donor, no significant current response was observed by application of 10 μM adenosine, 10 μM ATP or 3 mM Ba^{2+} (1.9 ± 0.7 nA, n = 6; 0.9 ± 0.6 nA, n = 6; 5.0 ± 1.3 nA, n = 10, respectively; Figure 1a). These results suggest that the adenosine-induced currents are mediated by GIRK channels. In addition, responses to adenosine were not observed in ND98 solution containing 98 mM Na^+ and no K^+ instead of the hK solution (n = 8; data not shown), suggesting that the currents show K^+ selectivity. The current-voltage relationship of the response to 3 μM adenosine showed strong inward rectification (Figure 1c), typical of a current response mediated by GIRK channels. In addition, similar results were obtained in oocytes injected with mRNAs for GIRK 1 and GIRK4 subunits (data not shown). These results suggest that an endogenous adenosine receptor can functionally couple to GIRK channels.

In the present study, although basally active GIRK currents sensitive to Ba^{2+} were observed in all oocyte batches injected with GIRK mRNAs, the successful responses to adenosine were observed in oocyte batches prepared from 14 of 56 donors (25.0%). The GIRK currents induced by 3 μM adenosine were variable among oocytes prepared from the same donor, and amplitudes of responses to adenosine were not significantly correlated with amplitudes of the 3 mM Ba^{2+}-sensitive current components (Figure 1d). Also, similar results were obtained in other oocyte batches from different donors (data not shown). In contrast, the unsuccessful responses to adenosine in oocytes prepared from most donors showed little or no inward current (11.9 ± 1.3 nA at 3 μM, n = 304), although amplitudes of the Ba^{2+}-sensitive current components, which are related to expression levels of GIRK channels (Kobayashi *et al.*, 2000), were large enough in the same oocytes (821.5 ± 58.7 nA, n = 304). Taken together, these results indicate that the expression level of an endogenous receptor for adenosine in defolliculated oocytes may be dependent on the oocyte batch from donors and may be variable from cell to cell among oocyte batches.

Pharmacological characteristics of a Xenopus *oocyte adenosine receptor*

To investigate the pharmacological characteristics of the *Xenopus* oocyte adenosine receptor found in the present study, we examined the effects of various adenosine receptor ligands in oocytes expressing GIRK channels. Two selective A_1 adenosine receptor agonists, CPA and N^6-cyclohexyladenosine (CHA), and a non-selective adenosine receptor agonist, 5'-(*N*-ethylcar-

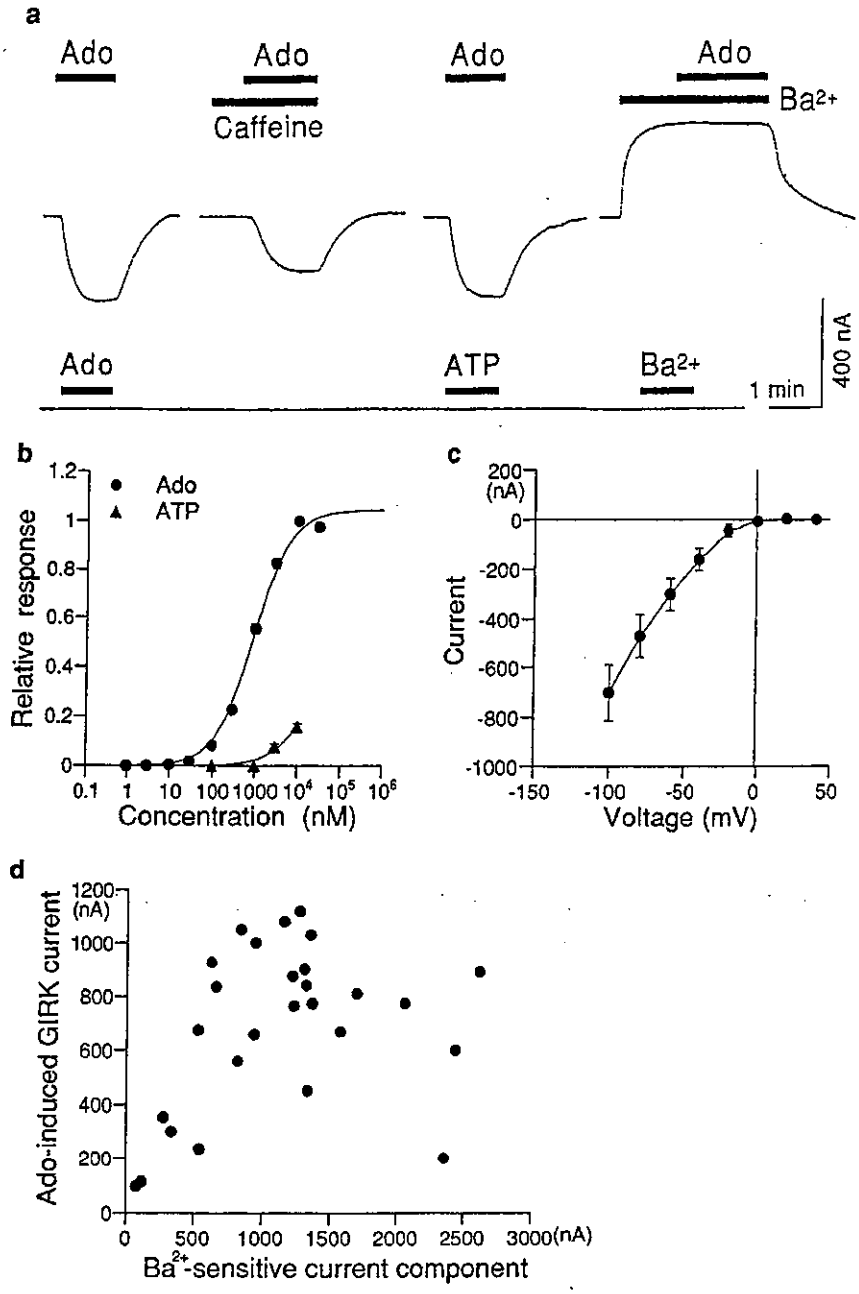

Figure 1 Effects of adenosine in *Xenopus* oocytes expressing GIRK channels. (a) Upper row, in a defolliculated oocyte injected with GIRK1 mRNA and GIRK2 mRNA, current responses to adenosine (Ado), Ado in the presence of 100 μM caffeine, Ado and Ado in the presence of 3 mM Ba^{2+} are shown. The concentration of Ado used was 3 μM. Lower row, in an uninjected oocyte, current responses to 10 μM Ado, 10 μM ATP and 3 mM Ba^{2+} are shown. Current responses were measured at a membrane potential of -70 mV in a high-potassium solution containing 96 mM K^+. Bars show the duration of application. (b) Concentration-response relationships for GIRK channel activation induced by Ado or ATP. Effects of these drugs were normalized to the magnitudes of 10 μM Ado-induced GIRK currents, which were 556.4 ± 64.0 nA ($n=20$). Each point and error bar represents the mean and s.e.mean of the relative responses obtained from 10 oocytes. Data points were fitted using a logistic equation. (c) Current-voltage relationship of 3 μM Ado-induced GIRK currents in oocytes expressing GIRK1/2 channels ($n=8$). (d) Correlation between the amplitudes of current response to 3 μM Ado and of the 3 mM Ba^{2+}-sensitive current component in oocytes prepared from the same donor. The correlation coefficient was 0.317 ($P>0.1$, $n=27$; correlation analysis).

boxaminido)adenosine (NECA), concentration-dependently induced inward current responses at nanomolar concentrations (Figure 2a,c and Table 1), whereas at the highest concentration used they induced no current response in uninjected oocytes ($n=5$; data not shown). The rank order of potency for these adenosine receptor agonists was CHA$\geqslant$CPA$>$NECA$>$adenosine, whereas the rank order of efficacy for these agonists was NECA$>$adenosine$>$CPA$>$CHA (Figure 2c and Table 1). The n_H values for the these adenosine receptor agonists were not significantly different from 1 (Student's t-test, $P>0.05$), suggesting a single site of action for each of the agonists. Furthermore, the current responses to 3 μM adenosine were

Table 1 Comparison of pharmacological characteristics of an endogenous *Xenopus* oocyte adenosine receptor and the cloned XA_1 receptor

	Xenopus *oocyte adenosine receptor*				*XA_1 receptor*			
Compound	*EC_{50}*	*Max. efficacy*	*n_H*	(n)	*EC_{50}*	*Max. efficacy*	*n_H*	(n)
Adenosine	917.3±69.4	1	0.88±0.02	(10)	2.91±0.54	1	0.83±0.11	(5)
CPA	96.7±10.1	0.81±0.03	0.91±0.03	(6)	5.72±0.87	1.03±0.01	0.99±0.03	(6)
CHA	86.7±28.3	0.65±0.02	0.89±0.04	(9)	3.60±0.89	1.11±0.04	0.96±0.07	(5)
NECA	398.6±117.9	1.70±0.20*	0.95±0.05	(5)	0.56±0.05	0.96±0.02	0.92±0.04	(5)
CGS21680	N.D.	N.D.	N.D.	(5)	205.6±20.3	0.87±0.03	0.90±0.04	(5)
IB-MECA	N.D.	N.D.	N.D.	(4)	135.2±12.8	0.96±0.04	0.97±0.02	(6)

The EC_{50} values are shown as mean±s.e.mean in nM. The values of maximal efficacy (Max. efficacy) were normalized to magnitude of GIRK currents induced by adenosine at 10 μM in an endogenous *Xenopus* oocyte adenosine receptor and at 1 μM in the XA_1 receptor. The n_H values indicate the mean±s.e.mean of the Hill coefficients. The numbers of oocytes tested are indicated in parentheses. N.D. means that these values were not determined because these compounds induced only small GIRK responses at micromolar concentrations. *The high efficacy raises the possibilities that NECA, a non-selective adenosine receptor agonist, may cause a distinct conformational change of the endogenous adenosine receptor and that there may be additional types of oocyte adenosine receptors which are activated not by A_1 adenosine receptor agonists but by NECA.

almost completely abolished by 1 μM DPCPX, a selective A_1 adenosine receptor antagonist, with an IC_{50} value of 18.0±2.6 nM and a n_H value of 0.96±0.07 (n=4, Figure 2a,d). However, a selective A_{2A} adenosine receptor agonist, 2-[*p*-(2-carbonyl-ethyl)-phenylethylamino]-5'-N-ethylcarboxamidoadenosine (CGS21680), and a selective A_3 adenosine receptor agonist, IB-MECA, produced only small current responses as compared with the responses to 10 μM adenosine (0% at 100 nM, 7.9±0.8% at 1 μM and 9.9±5.3% at 30 μM for CGS21680, n=5; 0% at 100 nM, 1.7±1.7% at 300 nM and 5.7±2.9% at 1 μM for IB-MECA, n=4, respectively). In addition, DMSO, the solvent vehicle, at the highest concentration (0.1%) used had no effect in this study.

As the present results indicated that characteristics of the adenosine receptor found here resembled those of the A_1 adenosine receptor, we next compared the receptor found with the XA_1 receptor identified in *Xenopus laevis* by Nebreda (GenBank/EMBL/DDBJ databases: accession number AJ249842). For functional characterization of the cloned XA_1 receptor, we first carried out molecular cloning of the cDNA from oocytes of *Xenopus laevis* and surrounding tissues by reverse transcription-PCR. The specific PCR product was detected by agarose gel electrophoresis and cloned as described previously (Ikeda *et al.*, 1995). The deduced amino acid sequence of the cDNA for the XA_1 receptor was identical with the reported sequence. The XA_1 receptor shares 72% and 72.5% amino acid sequence identity with the rat and human A_1 adenosine receptors, respectively, whereas the overall amino acid sequence identity for the A_1 adenosine receptor between the mammalian species is approximately 95%. To investigate functional coupling of the XA_1 receptor to GIRK channels and pharmacological characteristics of the receptor, we used oocytes co-injected with mRNAs for the XA_1 receptor and GIRK channels, when 3 μM adenosine induced no significant current response in oocytes from the same donor injected with GIRK mRNAs (75.0% of donors). Application of adenosine, CPA or CHA, at low nanomolar concentrations, induced significant inward currents with similarly high potency and similar efficacy (Figure 2b,c and Table 1). However, CGS21680 and IB-MECA induced current responses at relatively high nanomolar concentrations (Table 1). The responses to adenosine were attenuated in the presence of caffeine (IC_{50} value of 327.1±34.4 μM and n_H value of 0.89±0.10, n=4) and DPCPX (IC_{50} value of 56.4±5.2 nM and n_H value of 0.85±0.08, n=4) (Figure 2d). In oocytes injected with XA_1 receptor mRNA alone, 3 μM adenosine induced no significant current response (3.4±0.7 nA, n=8). These results indicate that the XA_1 receptor also couples to GIRK channels and the pharmacological properties of the XA_1 receptor are typical of the A_1 adenosine receptor, although the amino acid sequences for the XA_1 receptor and the mammalian A_1 adenosine receptors exhibit relatively low identity. In addition, the XA_1 receptor was fully activated by low nanomolar concentrations of adenosine, whereas such low concentrations of adenosine induced little or no response in all the oocyte batches injected with GIRK mRNAs (Figure 2c), suggesting that the XA_1 receptor may be located exclusively in follicle cells and outer surrounding tissues or only sparsely in the oocyte membrane. Further studies by *in situ* hybridization analysis and immunohistochemical analysis may identify the location of the XA_1 receptor. As shown in Figure 2c and Table 1, the potency and efficacy of adenosine, NECA and A_1 adenosine receptor agonists for the adenosine receptor found here are distinct from those of the XA_1 receptor. Moreover, the adenosine receptor found here was insensitive to micromolar concentrations of CGS21680 and IB-MECA, whereas the XA_1 receptor was sensitive to moderate nanomolar concentrations of these agonists. While the antagonist effects of caffeine and DPCPX, adenosine receptor antagonists tested, on the adenosine receptor found here and the XA_1 receptor were similar (Figure 2d). In addition, the characteristics of the XA_1 receptor were observed similarly even in the oocytes which showed similar magnitudes of GIRK current responses *via* the XA_1 receptor as compared with magnitudes of the responses *via* the endogenous adenosine receptor found here, suggesting that the differences in pharmacological characteristics between the endogenous adenosine receptor and the XA_1 receptor were not caused by differences in receptor density expressing in oocytes. The present results suggest that the endogenous adenosine receptor found in defolliculated oocytes is different from the XA_1 and A_3 adenosine receptors.

Signal transduction mechanisms of a Xenopus *oocyte adenosine receptor*

Activation of various GPCRs opens GIRK channels *via* direct action of G protein $\beta\gamma$-subunits ($G\beta\gamma$) released from

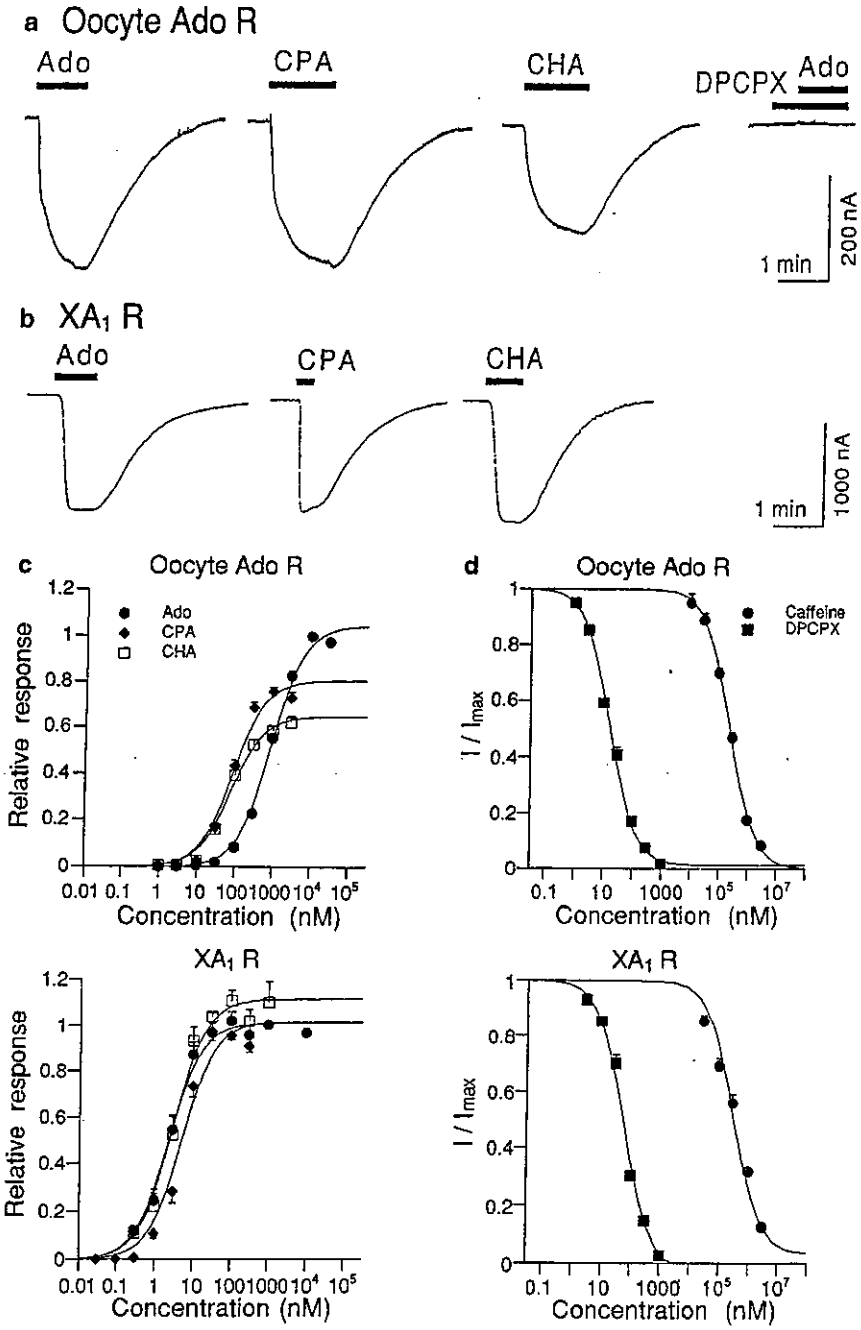

Figure 2 Effects of adenosine receptor ligands on an endogenous *Xenopus* oocyte adenosine receptor (Oocyte Ado R) and the cloned *Xenopus* adenosine A_1 receptor (XA_1 R). (a) In a defolliculated oocyte injected with GIRK1 and GIRK2 mRNAs, current responses to 3 μM Ado, 1 μM CPA, 1 μM CHA and 3 μM Ado in the presence of 1 μM DPCPX are shown. (b) In a defolliculated oocyte injected with mRNAs for the XA_1 receptor and GIRK1/2 channels, current responses to 100 nM Ado, 100 nM CPA and 100 nM CHA are shown. Bars show the duration of application. (c) Concentration-response relationships for adenosine receptor agonists on Oocyte Ado R (top) and XA_1 R (bottom). The magnitudes of GIRK currents induced by adenosine receptor agonists were normalized to the magnitudes of 10 μM Ado-induced currents, which were 355.9±36.7 nA (n=25), in oocytes injected with GIRK1 and GIRK2 mRNAs and to the magnitudes of 1 μM Ado-induced currents, which were 574.8±122.2 nA (n=16), in oocytes co-injected with mRNAs for the XA_1 receptor and GIRK1/2 channels, respectively. (d) Concentration-dependent inhibition of adenosine-induced currents by adenosine receptor antagonists on Oocyte Ado R (top) and XA_1 R (bottom). I_{max} is the amplitude of GIRK currents induced by Ado at 3 μM in Oocyte Ado R (563.1±91.2 nA, n=12) and at 10 nM in XA_1 R (325.7±77.7 nA, n=8), and I is the current amplitude in the presence of an adenosine receptor antagonist. Current responses were measured at a membrane potential of −70 mV in a high-potassium solution containing 96 mM K^+. Each point and error bar represents the mean and s.e.mean of the relative responses obtained from 4–10 oocytes. Data points were fitted using a logistic equation.

$G_{i/o}$ proteins, which are sensitive to PTX (Brown & Birnbaumer, 1990; Reuveny *et al.*, 1994). To investigate the involvement of G protein-coupled mechanisms in activation of GIRK channels by the endogenous adenosine receptor found here, the responses to adenosine in oocytes expressing GIRK 1/2 channels were compared with and without PTX injection. The current responses to adenosine were almost completely abolished by injection of PTX (Figure 3a). The current responses to adenosine in the PTX-injected oocytes were significantly different from those in the sham-injected oocytes (Figure 3a). These results indicate that the endogenous adenosine receptor opens GIRK channels *via* activation of $G_{i/o}$ proteins and is present on the oocyte membrane.

We next examined whether the receptor regulates intracellular cyclic AMP levels. In the defolliculated oocyte groups which showed the successful current responses to 3 μM adenosine in oocytes expressed with GIRK channels, CPA significantly reduced cyclic AMP accumulation stimulated by forskolin, which produced a modest increase in the cyclic AMP content by 32% (Student's *t*-test, $P<0.01$) in comparison with that of the untreated oocyte group (Figure 3b). Whereas CPA alone had no significant effect on cyclic AMP levels (Figure 3b). In contrast, the defolliculated oocyte groups which showed the unsuccessful current responses to adenosine in oocytes expressed with GIRK channels resulted in no significant change in cyclic AMP levels in any oocyte groups by addition of CPA (data not shown, five donors). The results suggest that the endogenous adenosine receptor inhibits adenylyl cyclase.

Discussion

In the present study we demonstrated that an endogenous *Xenopus* oocyte adenosine receptor on the oocyte membrane can activate GIRK channels expressed in oocytes *via* interaction with PTX-sensitive G proteins. Furthermore, the receptor inhibited forskolin-stimulated cyclic AMP accumulation. These results suggest the existence of a $G_{i/o}$ protein-coupled adenosine receptor in the oocyte.

Among the cloned adenosine receptor subtypes, the A_1 and A_3 adenosine receptors interact with $G_{i/o}$ proteins (Ralevic & Burnstock, 1998). We demonstrated that the adenosine receptor found here was sensitive to two A_1 adenosine receptor agonists with EC_{50} values of moderate nanomolar concentrations, whereas the receptor was insensitive to A_{2A} and A_3 adenosine receptor agonists tested (Figure 2c and Table 1). These results suggested that the receptor resembled an A_1 adenosine receptor. However, when compared with the cloned XA_1 receptor (Figure 2 and Table 1), the pharmacological characteristics of the adenosine receptor found here were distinct from those of the XA_1 receptor. Also, in the *Xenopus* oocyte system co-expressing the cloned rat A_1 adenosine receptor and GIRK channels, the receptor was fully activated by CPA and CGS21680 with EC_{50} values of 7 nM and 2.6 μM, respectively (Pfaff & Karschin, 1997). Therefore, our results suggest that the adenosine receptor found in this study is different from the four subtypes of cloned adenosine receptors reported to date.

In addition to the cloned adenosine receptors, physiological, pharmacological and biochemical studies have suggested the existence of additional adenosine receptors in the *Xenopus* oocyte and in several tissues in mammals. In *Xenopus* follicular oocytes (Lotan *et al.*, 1982; 1985; Miledi & Woodward, 1989; Greenfield *et al.*, 1990a, b) or defolliculated oocytes (Gelerstein *et al.*, 1988), adenosine elevates cyclic AMP levels, and elicits cyclic AMP-mediated outward K^+ currents with an EC_{50} value of approximately 3 μM, indicating that the receptors for adenosine stimulate adenylyl cyclase *via* G_s proteins and resemble A_2 adenosine receptors. In addition, King *et al.* (1996) demonstrated that adenosine and ATP produced similar outward K^+ currents in follicular oocytes with distinct pharmacological characteristics. The characteristics exhibited that adenosine and ATP were equipotent with EC_{50} values of 1.9 and 1.7 μM, respectively, whereas ATP and CGS21680 were 0.5 and 0.7 times as efficient as adenosine, respectively. However, we demonstrated that the adenosine receptor in defolliculated oocytes was coupled to $G_{i/o}$ proteins and inhibited folskolin-stimulated cyclic AMP accumulation and that the receptor was activated by adenosine with an EC_{50} value of 917.3 nM but insensitive to ATP and CGS21680 at micromolar concentrations (Figures 1b, 2c and 3 and Table 1). Finidori *et al.* (1982) showed that adenosine inhibited adenylyl cyclase activity in the defolliculated oocyte membrane fraction, suggesting that the effect may be mediated by interaction with $G_{i/o}$ proteins. However, only high micromolar concentrations of adenosine had such effect. Therefore, our results suggest that the *Xenopus* adenosine receptor found here is different from the *Xenopus* adenosine receptors described previously.

In the rat brain membrane, [^{3}H]-CV 1808 binding study under anomalously low temperature suggested the existence of a novel high affinity component that could only partially be displaced by classical adenosine receptor ligands including CPA and a low affinity component with A_1-like adenosine receptor characteristics (Cornfield *et al.*, 1992). Also, [^{3}H]-CV 1808 binding was not affected by 1 μM adenosine or GTP, and the IC_{50} values for NECA and DPCPX were greater than 10 μM. Later, Luthin & Linden (1995) demonstrated that receptors on membranes prepared from both rat brain and COS cells transfected with rat A_{2A} adenosine receptor took on either the unique binding characteristics of [^{3}H]-CV 1808 or the characteristics of A_{2A} adenosine receptor, depending on temperature of the binding assay and the nature of the radioligand. We demonstrated that the receptor found here was sensitive to adenosine, NECA and DPCPX at nanomolar concentrations, and also coupled to $G_{i/o}$ proteins, indicating that the characteristics of the receptor found here are distinct from those of [^{3}H]-CV 1808 binding sites. Like the receptor found here, studies on the inhibitory effect on noradrenaline release in sympathetic nerves of the rat caudal artery (Shinozuka *et al.*, 1988) and rat vas deferens (Forsyth *et al.*, 1991) and in the rabbit brain cortex (von Kügelgen *et al.*, 1992) suggested the existence of putatively novel receptors activated by adenosine and ATP, and antagonized by xanthine derivatives. In the sympathetic nerves, adenosine and ATP were equipotent with EC_{50} values of approximately 10 μM, whereas in the brain, adenosine was more potent than ATP but both drugs were equally effective at 3 μM. In this study, adenosine was more potent than ATP and adenosine at 3 μM was much more efficacious than ATP, suggesting that the receptor found here is distinct from these receptors. In

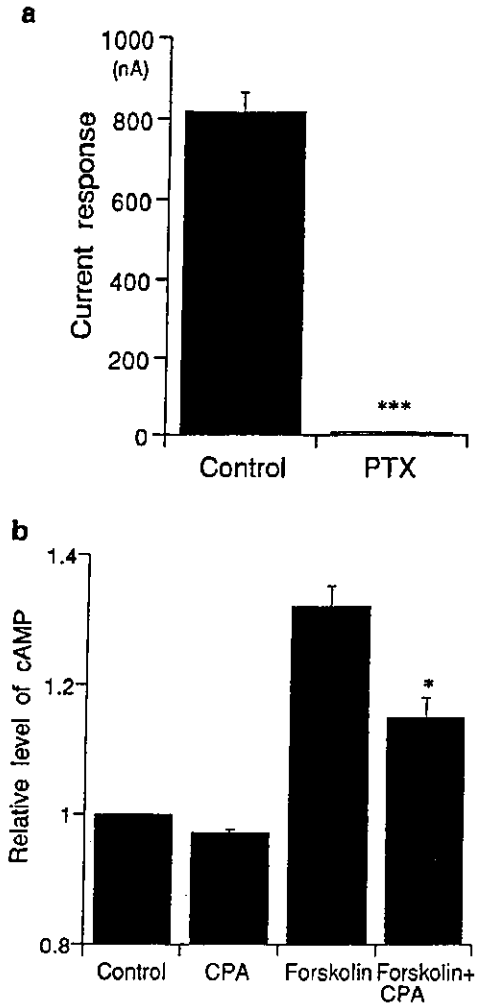

Figure 3 Interaction of an endogenous *Xenopus* oocyte adenosine receptor with $G_{i/o}$ proteins. (a) Effects of pertussis toxin (PTX) on adenosine-induced GIRK currents in oocytes expressing GIRK channels. The relationship of current responses to 3 μM adenosine (Ado) between the PTX-untreated group (817.9±48.0 nA; $n=14$; black bar) and PTX-treated group (8.46±2.65 nA; $n=22$; open bar). Current responses were measured at a membrane potential of −70 mV in a high-potassium solution containing 96 mM K^+. (b) Effects of CPA on forskolin-stimulated cyclic AMP accumulation in oocytes. Groups of 25 oocytes were exposed to either 1 μM CPA or 30 μM forskolin, or both drugs for 30 min. The results were obtained from four separate experiments. The basal cyclic AMP level in control group of untreated oocytes was 2389±54 fmol oocyte^{-1}. The ratios of cyclic AMP levels in the oocyte groups treated with CPA, forskolin or forskolin and CPA to the control group were 0.97±0.01, 1.32±0.03 and 1.15±0.03, respectively. There was significant difference in cyclic AMP contents between the group treated with forskolin and the group treated with forskolin and CPA. Statistical analysis of differences between groups was carried out using Student's *t*-test. Asterisks indicate significant differences between groups ($^*P<0.05$; $^{***}P<0.001$).

addition, a study on relaxation of smooth muscle in the porcine coronary artery suggested the existence of another type of adenosine receptor (Abebe *et al.*, 1994). However, the receptor was insensitive to xanthines and the receptor-mediated vasorelaxation was independent of the effects mediated by CPA and CHA. Therefore, we propose the existence of an endogenous *Xenopus* oocyte adenosine receptor with unique pharmacological characteristics distinct from those of known subtypes of adenosine receptors and other proposed adenosine receptors. The receptor may be considered an A_1-like adenosine receptor, although the nomenclature of the newly proposed receptors including the adenosine receptor found in this study remains tentative until identification of the adenosine receptors with the unique pharmacological characteristics.

The coronary vasodilatation mediated by 1 μM adenosine was attenuated by antidiabetic sulfonylureas (Daut *et al.*, 1990) and 10 μM adenosine or 100 nM CHA activated the ATP-sensitive K^+ channels, which are blocked by sulfonylureas, *via* $G_i\alpha$ proteins in rat ventricular myocytes (Kirsch *et al.*, 1990), but the pharmacological characteristics of adenosine receptor agonists were not reported in these studies. The results suggested that an adenosine receptor sensitive to an A_1 adenosine receptor agonist couples to the ATP-sensitive K^+ channels *via* G_i proteins. Further studies using cDNA clones for ATP-sensitive K^+ channels (Ho *et al.*, 1993; Inagaki *et al.*, 1995a,b) may clarify whether the adenosine receptor found here can activate the K^+ channels.

Endogenous *Xenopus* oocyte GIRK-related polypeptides (XIR) are also located on the oocyte membrane, although levels of XIR expression are low and variable among oocyte batches from different donors (Duprat *et al.*, 1995; Hedin *et al.*, 1996). As adenosine induced no significant current response in any of the naive defolliculated oocytes tested, the *Xenopus* adenosine receptor found here may hardly have XIR effect. However, the endogenous receptor was activated by adenosine at nanomolar concentrations, which are estimated to be in the physiological range of extracellular fluid (Fredholm, 1995). Therefore, other intracellular signal pathways *via* $G_{i/o}$ proteins may be involved in some effects in oocyte physiology.

Gelerstein *et al.* (1988) demonstrated in experiments using follicular oocytes and oocytes defolliculated by collagenase treatment and shaking periodically that 10 μM adenosine induced maturation, which was assessed by germinal vesicle breakdown, in stage VI oocytes and accelerated maturation of stage V and VI oocytes induced by approximately 3 μM progesterone. Also, adenosine increased cyclic AMP in defolliculated oocytes to the same extent as in follicular oocytes, suggesting interaction of an adenosine receptor located on the oocyte membrane with G_s proteins. In contrast, cyclic AMP is produced in follicle cells in response to NECA but no cyclic AMP accumulation can be detected in oocytes stripped by manual dissection after hypertonic treatment of collagenase-treated follicles, indicating that the receptor for adenosine appears to be located exclusively on follicle cells (Greenfield *et al.*, 1990b). Despite localization of the endogenous G_s protein-coupled adenosine receptor, signal transduction by a $G_{i/o}$ protein-coupled adenosine receptor found here as well as that by the G_s protein-coupled adenosine receptor may have some effects on numerous biochemical events in oocyte maturation. Recently, Lutz *et al.* (2000) demonstrated that *Xenopus* oocyte maturation induced by 50 nM progesterone was inhibited by $G\beta_1\gamma_2$, which can directly activate GIRK channels (Reuveny *et al.*, 1994). Activation of GIRK channels by the adenosine receptor found in this study may be mediated by action of $G\beta\gamma$ released from *Xenopus* $G_{i/o}$ proteins. The existence of the receptor may affect the signal transduction pathway induced by progesterone. Identification of the adenosine receptor

found here by molecular biological and genetic approaches may facilitate clarification of the functions and expression mechanisms of the receptor in *Xenopus* oocyte maturation.

In conclusion, we demonstrate that an endogenous *Xenopus* adenosine receptor on the oocyte membrane couples to GIRK channels and adenylyl cyclase *via* interaction with $G_{i/o}$ proteins. Moreover, the unique pharmacological characteristics of the receptor may suggest the existence of a putatively novel adenosine receptor. As the receptor was activated by nanomolar concentrations of adenosine, which is a normal constituent of extracellular fluid, $G_{i/o}$ protein signaling pathways *via* the adenosine receptor may have some effects in ovarian physiology.

We thank Dr Kansaku Baba for cooperation, and Mr Tomio Ichikawa and Mr Kazuo Kobayashi for their assistance. This work was supported by research grants from the Ministry of Education, Culture, Sports, Science and Technology of Japan, the Cooperative Research Program of the RIKEN Brain Science Institute, Japan Society for the Promotion of Science and Nakayama Foundation for Human Science.

References

ABEBE, W., MAKUJINA, S.R. & MUSTSFA, S.J. (1994). Adenosine receptor-mediated relaxation of porcine coronary artery in presence and absence of endothelium. *Am. J. Physiol.*, **266**, H2018–H2025.

BROWN, A.M. & BIRNBAUMER, L. (1990). Ionic channels and their regulation by G protein subunits. *Annu. Rev. Physiol.*, **52**, 197–213.

COLLIS, M.G. & HOURANI, S.M.O. (1993). Adenosine receptor subtypes. *Trends Pharmacol. Sci.*, **14**, 360–366.

CORNFIELD, L.J., HU, S., HURT, S.D. & SILLS, M.A. (1992). [^{3}H]2-phenylaminoadenosine ([^{3}H]CV 1808) labels a novel adenosine receptor in rat brain. *J. Pharmacol. Exp. Ther.*, **263**, 552–561.

DASCAL, N. (1987). The use of *Xenopus* oocytes for the study of ion channels. *CRC Crit. Rev. Biochem.*, **22**, 317–387.

DASCAL, N., SCHREIBMAYER, W., LIM, N.F., WANG, W., CHAVKIN, C., DIMAGNO, L., LABARCA, C., KIEFFER, B.L., GAVERIAUX-RUFF, C., TROLLINGER, D., LESTER, H.A. & DAVIDSON, N. (1993). Atrial G protein-activated K^+ channel: Expression cloning and molecular properties. *Proc. Natl. Acad. Sci. U.S.A.*, **90**, 10235–10239.

DAUT, J., MAIER-RUDOLPH, W., VON BEKERATH, N., MEHRKE, G., GUNTHER, K. & GOEDEL-MEIDEN, L. (1990). Hypoxic dilation of coronary arteries is mediated by ATP-sensitive potassium channels. *Science*, **247**, 1341–1344.

DUPRAT, F., LESAGE, F., GUILLEMARE, E., FINK, M., HUGNOT, J.-P., BIGAY, J., LAZDUNSKI, M., ROMEY, G. & BARHANIN, J. (1995). Heterologous multimeric assembly is essential for K^+ channel activity of neuronal and cardiac G-protein-activated inward rectifiers. *Biochem. Biophys. Res. Commun.*, **212**, 657–663.

FINIDORI, J., HANOUNE, J. & BAULIEU, E.E. (1982). Adenylate cyclase in *Xenopus laevis* oocytes: characterization of the progesterone-sensitive, membrane-bound form. *Mol. Cell. Endocrinol.*, **28**, 211–227.

FORSYTH, K.N., BJUR, R.A. & WESTFALL, D.P. (1991). Nucleotide modulation of norepinephrine release from sympathetic nerves in the rat vas deferens. *J. Pharmacol. Exp. Ther.*, **256**, 821–826.

FRASER, S.P. & DJAMGOZ, M.B.A. (1992). *Xenopus* oocytes: endogenous electrophysiological characteristics. In *Current Aspects of the Neurosciences*, vol. 4. ed. Osborne, N. N. pp. 267–315. London: Macmillan Press.

FREDHOLM, B.B. (1995). Adenosine, adenosine receptors and the actions of caffeine. *Pharmacol. Toxicol.*, **76**, 93–101.

GELERSTEIN, S., SHAPIRA, H., DASCAL, N., YEKUEL, R. & ORON, Y. (1988). Is a decrease in cyclic AMP a necessary and sufficient signal for maturation of Amphibian oocytes? *Dev. Biol.*, **127**, 25–32.

GREENFIELD, JR., L.J., HACKETT, J.T. & LINDEN, J. (1990a). *Xenopus* oocyte K^+ current. I. FSH and adenosine stimulated follicle cell-dependent currents. *Am. J. Physiol.*, **259**, C775–C783.

GREENFIELD JR., L.J., HACKETT, J.T. & LINDEN, J. (1990b). *Xenopus* oocyte K^+ current. II. Adenylyl cyclase-linked receptors on follicle cells. *Am. J. Physiol.*, **259**, C784–C791.

HEDIN, K.E., LIM, N.F. & CLAPHAM, D.E. (1996). Cloning of a Xenopus laevis inwardly rectifying K^+ channel subunit that permits GIRK1 expression of I_{KACh} currents in oocytes. *Neuron*, **16**, 423–429.

HO, K., NICHOLS, C.G., LEDERER, W.J., LYTTON, J., VASSILEV, P.M., KANAZIRSKA, M.V. & HEBERT, S.C. (1993). Cloning and expression of an inwardly rectifying ATP-regulated potassium channel. *Nature*, **362**, 31–38.

IKEDA, K., KOBAYASHI, K., KOBAYASHI, T., ICHIKAWA, T., KUMANISHI, T., KISHIDA, H., YANO, R. & MANABE, T. (1997). Functional coupling of the nociceptin/orphanin FQ receptor with the G-protein-activated K^+ (GIRK) channel. *Mol. Brain Res.*, **45**, 117–126.

IKEDA, K., KOBAYASHI, T., ICHIKAWA, T., KUMANISHI, T., NIKI, H. & YANO, R. (2001). The untranslated region of μ-opioid receptor mRNA contributes to reduced opioid sensitivity in CXBK mice. *J. Neurosci.*, **21**, 1334–1339.

IKEDA, K., KOBAYASHI, T., ICHIKAWA, T., USUI, H., ABE, S. & KUMANISHI, T. (1996). Comparison of the three mouse G-protein-activated K^+ (GIRK) channels and functional couplings of the opioid receptors with the GIRK1 channel. *Ann. NY. Acad. Sci.*, **801**, 95–109.

IKEDA, K., KOBAYASHI, T., ICHIKAWA, T., USUI, H. & KUMANISHI, T. (1995). Functional couplings of the δ- and the κ-opioid receptors with the G-protein-activated K^+ channel. *Biochem. Biophys. Res. Commun.*, **208**, 302–308.

INAGAKI, N., GONOI, T., CLEMENT, J.P. IV, NAMBA, N., INAZAWA, J., GONZALEZ, G., AGUILAR-BRYAN, L., SEINO, S. & BRYAN, J. (1995a). Reconstitution of I_{KATP}: an in ward rectifier subunit plus the sulfonylurea receptor. *Science*, **270**, 1166–1170.

INAGAKI, N., TSUURA, Y., NAMBA, N., MASUDA, K., GONOI, T., HORIE, M., SEINO, Y., MIZUTA, M. & SEINO, S. (1995b). Cloning and functional characterization of a novel ATP-sensitive potassium channel ubiquitously expressed in rat tissues, including pancreatic islets, pituitary, skeletal muscle, and heart. *J. Biol. Chem.*, **270**, 5691–5694.

KING, B.F., PINTOR, J., WANG, S., ZIGANSHIN, A.U., ZIGANSHINA, L.E. & BURNSTOCK, G. (1996). A novel P_1 purinoceptor activates an outward K^+ current in follicular oocytes of *Xenopus laevis*. *J. Pharmacol. Exp. Ther.*, **276**, 93–100.

KIRSCH, G.E., CODINA, J., BIRNBAUMER, L. & BROWN, A.M. (1990). Coupling of ATP-sensitive K^+ channels to A_1 receptors by G proteins in rat ventricular myocytes. *Am. J. Physiol.*, **259**, H820–H826.

KOBAYASHI, T., IKEDA, K., ICHIKAWA, T., ABE, S., TOGASHI, S. & KUMANISHI, T. (1995). Molecular cloning of a mouse G-protein-activated K^+ channel (mGIRK1) and distinct distributions of three GIRK (GIRK1, 2 and 3) mRNAs in mouse brain. *Biochem. Biophys. Res. Commun.*, **208**, 1166–1173.

KOBAYASHI, T., IKEDA, K., KOJIMA, H., NIKI, H., YANO, R., YOSHIOKA, T. & KUMANISHI, T. (1999). Ethanol opens G-protein-activated inwardly rectifying K^+ channels. *Nat. Neurosci.*, **2**, 1091–1097.

KOBAYASHI, T., IKEDA, K. & KUMANISHI, T. (1998). Effects of clozapine on the δ- and κ-opioid receptors and the G-protein-activated K^+ (GIRK) channel expressed in *Xenopus* oocytes. *Br. J. Pharmacol.*, **123**, 421–426.

KOBAYASHI, T., IKEDA, K. & KUMANISHI, T. (2000). Inhibition of various antipsychotic drugs on the G-protein-activated inwardly rectifying K^+ (GIRK) channels expressed in *Xenopus* oocytes. *Br. J. Pharmacol.*, **129**, 1716–1722.

LOTAN, I., DACAL, N., COHEN, S. & LASS, Y. (1982). Adenosine-induced slow ionic currents in the *Xenopus* oocyte. *Nature*, **298**, 572–574.

LOTAN, I., DACAL, N., ORON, Y., COHEN, S. & LASS, Y. (1985). Adenosine-induced K^+ current in *Xenopus* oocyte and the role of adenosine 3',5'-monophosphate. *Mol. Pharmacol.*, **28**, 170–177.

LUTHIN, D.R. & LINDEN, J. (1995). Comparison of A_4 and A_{2a} binding sites in striatum and COS cells transfected with adenosine A_{2a} receptors. *J. Pharmacol. Exp. Ther.*, **272**, 511–518.

LUTZ, L.B., KIM, B., JAHANI, D. & HAMMES, S.R. (2000). G protein $\beta\gamma$ subunits inhibit nongenomic progesterone-induced signaling and maturation in *Xenopus laevis* oocytes. Evidence for a release of inhibition mechanism for cell cycle progression. *J. Biol. Chem.*, **275**, 41512–41520.

MILEDI, R. & WOODWARD, R.M. (1989). Effects of defolliculation on membrane current responces of *Xenopus* oocytes. *J. Physiol.*, **416**, 601–621.

NORTH, R.A. (1989). Drug receptors and the inhibition of nerve cells. *Br. J. Pharmacol.*, **98**, 13–28.

NYCE, J.W. (1999). Insight into adenosine receptor function using antisense and gene-knockout approches. *Trends Pharmacol. Sci.*, **120**, 79–83.

PFAFF, T. & KARSCHIN, A. (1997). Expression cloning of rat cerebellar adnosine A1 receptor by coupling to Kir channels. *NeuroReport*, **8**, 2455–2460.

POULSEN, S.-A. & QUINN, R.J. (1998). Adenosine receptors: new opportunities for future drugs. *Bioorg. Med. Chem.*, **6**, 619–641.

RALEVIC, V. & BURNSTOCK, G. (1998). Receptors for purines and pyrimidines. *Pharmacol. Rev.*, **50**, 413–492.

REUVENY, E., SLESINGER, P.A., INGLESE, J., MORALES, J.M., INIGUEZ-LLUHI, J.A., LEFKOWITZ, R.J., BOURNE, H.R., JAN, Y.N. & JAN, L.Y. (1994). Activation of the cloned muscarinic potassium channel by G protein $\beta\gamma$ subunits. *Nature*, **370**, 143–146.

SHINOZUKA, K., BJUR, R.A. & WESTFALL, D.P. (1988). Characterization of prejunctional purinoceptors on adrenergic nerves of the rat caudal artery. *Naunyn-Schmiedeberg's Arch. Pharmacol.*, **338**, 221–227.

VON KÜGELGEN, I., SPATH, L. & STARKE, K. (1992). Stable adenine nucleotides inhibit [^{3}H]-noradrenaline release in rabbit brain cortex slices by direct action at presynaptic adenosine A_1-receptors. *Naunyn-Schmiedeberg's Arch. Pharmacol.*, **346**, 187–196.

(Received June 4, 2001
Revised October 29, 2001
Accepted October 31, 2001)

European Journal of Neuroscience, Vol. 16, pp. 565–574, 2002

Degeneration of pontine mossy fibres during cerebellar development in weaver mutant mice

Miwako Ozaki,[1] Tsutomu Hashikawa,[2] Kazutaka Ikeda,[1] Yukie Miyakawa,[1] Tomio Ichikawa,[3] Yoshihiro Ishihara,[4] Toshiro Kumanishi[3] and Ryoji Yano[1]
[1]Laboratory for Cellular Information Processing, Brain Science Institute (BSI), Riken, Wako, Saitama 351-0198, Japan
[2]Laboratory for Neural Architecture, Brain Science Institute (BSI), Riken, Wako, Saitama 351-0198, Japan
[3]Department of Molecular Neuropathology, Brain Research Institute, Niigata University, Niigata, Niigata 951-8585, Japan
[4]Department of Neuropathology, Tokyo Metropolitan Institute for Neuroscience, Fuchu, Tokyo 183-0042, Japan

Keywords: cerebellum, GIRK2, lobule formation, pontine nuclei

Abstract

In weaver mutant mice, substitution of an amino acid residue in the pore region of GIRK2, a subtype of the G-protein-coupled inwardly rectifying K^+ channel, changes the properties of the homomeric channel to produce a lethal depolarized state in cerebellar granule cells and dopaminergic neurons in substantia nigra. Degeneration of these types of neurons causes strong ataxia and Parkinsonian phenomena in the mutant mice, respectively. On the other hand, the mutant gene is also expressed in various other brain regions, in which the mutant may have effects on neuronal survival. Among these regions, we focused on the pontine nuclei, the origin of the pontocerebellar mossy fibres, projecting mainly into the central region of the cerebellar cortex. The results of histological analysis showed that by P9 the number of neurons in the nuclei was reduced in the mutant to about one half and by P18 to one third of those in the wild type, whereas until P7 the number were about the same in wild-type and weaver mutant mice. Three-dimensional reconstruction of the nuclei showed a marked reduction in volume and shape of the mutant nuclei, correlating well with the decrease in neuronal number. In addition, DiI (a lipophilic tracer dye) tracing experiments revealed retraction of pontocerebellar mossy fibres from the cerebellar cortex after P5. From these results, we conclude that projecting neurons in the pontine nuclei, as well as cerebellar granule cells and dopaminergic neurons in substantia nigra, strongly degenerate in weaver mutant mice, resulting in elimination of pontocerebellar mossy fibres during cerebellar development.

Introduction

Among the ataxic mutant mice, the weaver mutant has been studied extensively (Herrup, 1996; Hess, 1996). The causal mutation was mapped in *GIRK2* gene encoding an inwardly rectifying K^+ channel subunit (Patil *et al.*, 1995). Homomeric mutant channels lose their selectivity for K^+ ions and regulation by G-proteins, while heteromeric channels with GIRK1 keep their original properties in their ion selectivity and activity regulation (Kofuji *et al.*, 1996; Navarro *et al.*, 1996; Slesinger *et al.*, 1996; Hou *et al.*, 1999). The mutation produces neuronal degeneration in the cerebellum and substantia nigra which, respectively, result in a strong ataxia and Parkinsonian-type deficiencies. Strong expression of the mutant gene induces neuronal cell death in 80–90% of the cerebellar granule cells during their postmitotic and premigratory stages, leading to a severe reduction in the size of the entire cerebellar cortex. In addition, along the rostrocaudal axis, clear transverse boundaries of the strong degeneration have been observed at the rostral face of lobule VI and the caudal side of lobule IX (Herrup & Kuemerle, 1997; Eisenman *et al.*, 1998; Eisenman, 2000). Between these boundaries, the central region (lobules VI to IX) shows immature morphologies, i.e. smaller size and incomplete formation of sublobular structures.

Correspondence: Dr Ryoji Yano, as above.
E-mail: ryano@postman.riken.go.jp

Received 5 March 2002, revised 24 May 2002, accepted 10 June 2002

doi:10.1046/j.1460-9568.2002.02111.x

Cerebellar cortex is roughly separated to three regions, according to the origins of their major afferent mossy fibres (Voogd, 1995; Altman & Bayer, 1997). The anterobasal and anterodorsal lobes mainly receive afferents from the spinal cord, while the central and posterior lobes mainly receive the fibres from the pontine nuclei. The inferior lobe is a main recipient region of mossy fibres originating from the vestibular nuclei. Concerning the relationship between precerebellar systems and cerebellar cortex in weaver mutant mice, the mossy fibre systems and their origins have already been examined (Arsenio Nunes *et al.*, 1988; Baurle & Guldin, 1998). From the results of WGA-HRP (wheat germ agglutinin–horseradish peroxidase conjugate) tracing experiments, almost normal topographic organization of the spinocerebellar projection was found in the mutant mice (Arsenio Nunes *et al.*, 1988). In the vestibular nuclei, there were no significant changes in the number or morphology of neurons in weaver mutant compared to wild-type mice (Baurle & Guldin, 1998). On the other hand, no detailed analysis has been made of the mossy fibre afferents into the central region (the central and posterior lobes) and their origin, the pontine nuclei.

By *in situ* hybridization analysis, it has been shown that the *GIRK2* gene is strongly expressed in pontine nuclei during all developmental stages of the cerebellum, starting at late embryonic days (E16–18) through to adult, while the expression of *GIRK1* or *GIRK3* is weak or starts later during development (Kobayashi *et al.*, 1995; Chen *et al.*, 1997; Wei *et al.*, 1997). This expression pattern of *GIRK*s suggests

the formation of homomeric GIRK2 channels in pontine nuclei during development. Considering this together with the relatively severe degeneration of the central region in the cortex, the main receptive field of the pontocerebellar projections, we examined structural features of pontine nuclei and their projections in weaver mutants.

Materials and methods

Mouse strains

For establishment of the C3H weaver mice used in the present experiments, original weaver mutant mice obtained from Jackson Laboratory (ME, USA) were mated with inbred C3H Heston N mice (SLC, Japan) and backcrossed over three times (Kobayashi *et al.*, 1999).

In situ *hybridization of the whole brain and pontine nucleus*

The probe for GIRK2 mRNA was oligo GIRK2A, as described in the previous report (Kobayashi *et al.*, 1995). The probe was complementary to a 5′ end part of the mRNA, which contained a unique sequence of the *GIRK2* gene. The probe was 3′ end labelled with [^{35}S]-dATP (Amersham Pharmacia Biotech UK Inc., UK) using a terminal deoxyribonucleotidyl transferase kit (Takara Shuzo Inc., Japan). Tissue specimens were obtained from C3H/HeSlc mice and weaver mice at P7 and adult (2 months old) under deep diethyl-ether anaesthesia. Parasagittal and coronal sections of the specimens (15 μm in thickness) were prepared, prehybridized for 3 h at 42 °C in a prehybridization solution, and hybridized for 16 h at 42 °C. The

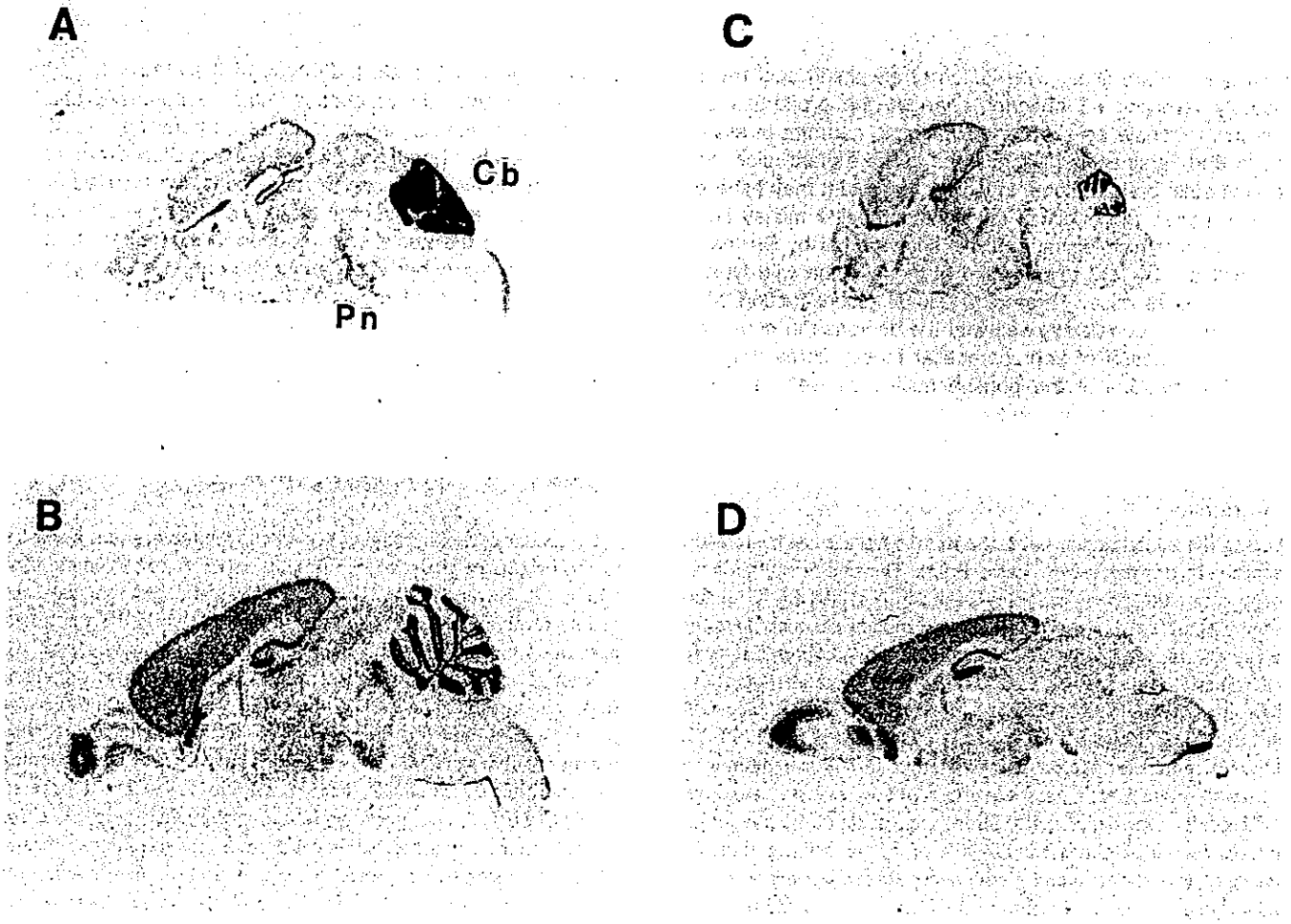

FIG. 1. Expression of GIRK2 mRNAs in P7 and adult mouse brains. Images were obtained after *in situ* hybridization of P7 and adult (2 months old) brain parasagittal sections of C3H wild-type and weaver mutant mice with probes specific for GIRK2 mRNA. (A) Wild type, P7. (B) Wild type, adult. (C) Weaver, P7. (D) Weaver, adult. The expression pattern of GIRK2 mRNA in the cerebellum and pontine nuclei of weaver mouse obviously differed from that of wild-type control. Cb, cerebellum; Pn, pontine nuclei.

FIG. 2. Distribution of GIRK2 mRNA in the pontine nuclei. Coronal sections were obtained from both wild-type and weaver mutant mice. Expression patterns of GIRK2 mRNA in the pontine nuclei were detected by *in situ* hybridization. (A and B) Wild type, P7. (C and D) Weaver, P7. (E and F) Wild type, adult. (G and H) Weaver, adult. A, C, E and G show dark-field micrographs and B, D, F and H show bright-field micrographs. After hybridization with labelled probes, tissue sections were autoradiographed using NTB2 nuclear track emulsion. Hybridized sections were counterstained with pyronin–methylgreen. Distinct signals of GIRK2 mRNA were observed in large neurons.

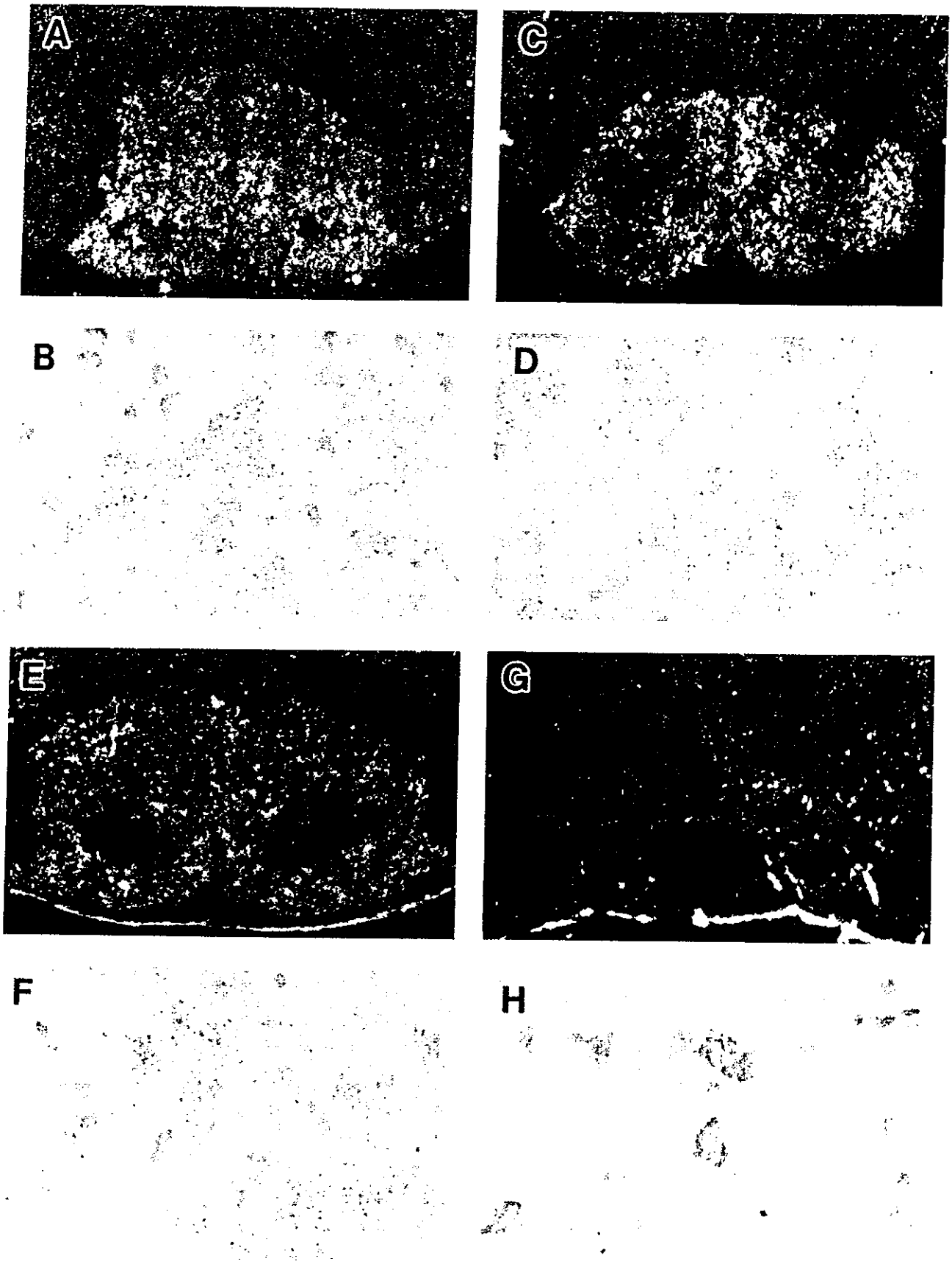
A
C
B
D
E
G
F
H

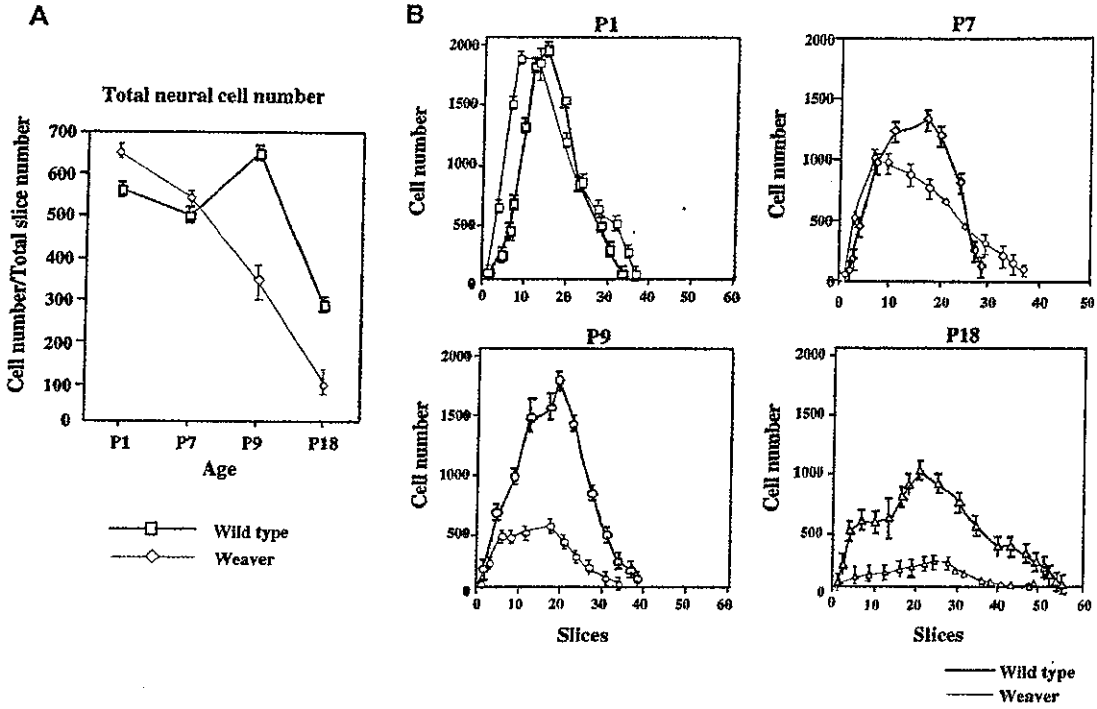

FIG. 3. Changes in the numbers of neurons in the pontine nuclei during development. The numbers of neurons were counted in 20-μm-thick serial sections of C3H wild-type and weaver mutant mouse brains during development (P1, P7, P9 and P18). Slices are numbered from rostral to caudal ends.

tissue sections were washed three times in 0.1 × SSC/0.1% Sarcosyl at 42 °C for 40 min, dehydrated and autoradiographed using Hyperfilm-βmax (Amersham Pharmacia Biotech) for 2 weeks to obtain images. In some cases, the sections were dipped into NTB2 emulsion (Kodak, USA), kept in the dark for a month and counterstained by pyronin–methylgreen after hybridization.

Counting the number of neurons and 3-D reconstruction of pontine nuclei

Coronal sections of postnatal day (P)1, P7, P9 and P18 were prepared from wild-type and weaver mutant mice as serial sections of 20 μm thickness and stained with pyronin–methylgreen. Neurons of pontine nuclei were plotted and counted using MD plot (Minnesota datametrics, MN, USA). Three-dimensional structure of the nuclei was reconstructed by using Strata Vision 3d (Strata Inc., USA).

DiI labelling of mossy fibres and tracing of the projection pattern

Under deep ether anaesthesia, developing mice (P0, P1, P3, P5, P7, P9, P14 and P18) were perfused with saline followed by a fixative containing 4% paraformaldehyde in 0.1 M phosphate buffer (pH 7.3). The brains were removed from skulls and immersed in phosphate-buffered 4% paraformaldehyde where they remained for 1–3 weeks. Then, with the aid of a small needle, pieces of crystals of DiI (a lipophilic tracer dye; Molecular Probes, Inc., OR, USA) were placed at the dorsal portion of the brachium pontis to label mossy fibres arising from the pontine nuclei. Following dye deposit the brains were returned to the fixative and stored in the dark at room temperature for 3 months before sectioning. Cerebellar cortices were sectioned in the parasagittal or coronal plane at 200 μm using vibroslicer (Microslicer DTK-1500, Dosaka EM Co. Ltd, Japan). The sections were collected in 0.1 M phosphate buffer and observed with a laser confocal microscope using YHS filter system (Bio-Rad Inc., CA, USA). The number of mossy fibre terminals was counted in weaver mutant and wild-type mice to make a map of the distribution on the cerebellar surface.

Experiments on animals

All animal experiments were carried out in accordance with the National Institute of Health Guide for the Care and Use of Laboratory Animals (NIH Publications no. 80–23) revised 1996, and all efforts were made to minimize the number of animals used.

Results

Expression intensity of GIRK2 gene in pontine nuclei was significantly reduced in adult weaver mutant mice

To observe the effects of the weaver mutation on the expression of its own gene, GIRK2, mRNA expression patterns were compared between the wild-type and mutant brains with the *in situ* hybridization method (Fig. 1). At P7, strong expression was found in the external and internal granular layers of wild-type cerebellum (Fig. 1A) while, in adults, the signals were detected only in the internal granular layer (Fig. 1B). In weaver mutant mice, however, the expression was observed only in the external granular layer at P7 (Fig. 1C), and no signal was detected in adult cerebellum (Fig. 1D). The absence of signals was consistent with the previous observation showing the granule cell death in the postmitotic stage before starting migration in the mutant (Rakic & Sidman, 1973a,b).

In the pontine nuclei, the signals were strongly detected at both P7 and adult in wild-type mice (Fig. 1A and B). However, the size of areas with positive signals was significantly reduced in adult weaver mutant mice compared with wild-type animals (Fig. 1C and D). The detailed distribution pattern of signals was observed in coronal sections of the nuclei from wild-type and weaver mutant mice

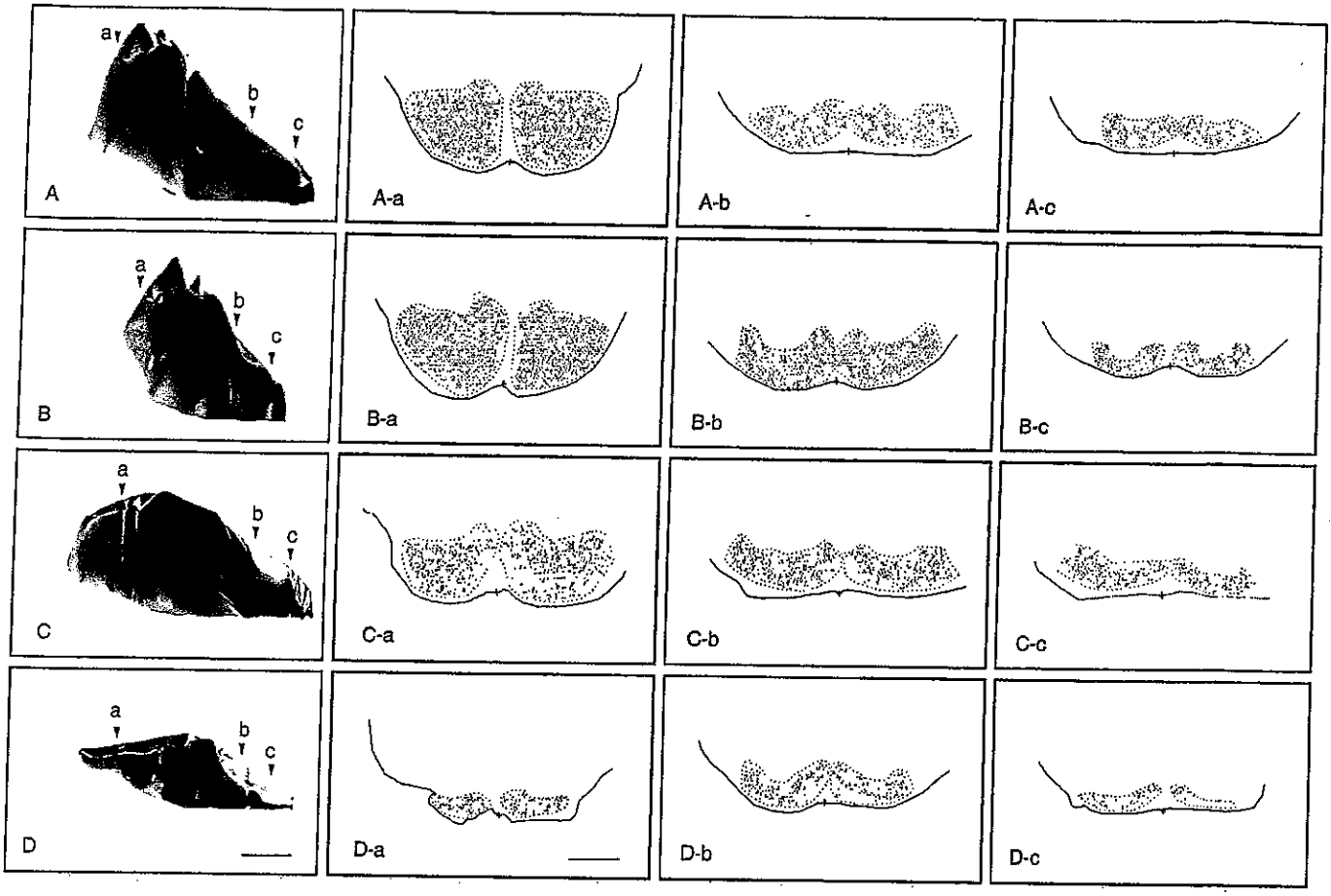

FIG. 4. Three-dimensional structure of the pontine nuclei and distribution of large neurons on sections. Coronal sections were prepared serially and stained with pyronin–methylgreen. After staining, the boundary of the pontine nuclei was traced with MD plot. Three-dimensional structure was reconstructed from the data of each section by using Strata Vision 3d software. Side views of the reconstructed pontine nuclei are shown in the left column. The rostrocaudal axis is orientated from left to right. (A) Wild type, P7. (B) Weaver, P7. (C) Wild type, P18. (D) Weaver, P18. Arrow heads (a–c) show position of each section in which distribution of neurons is shown. Scale bar, 300 μm.

(Fig. 2). Expression patterns of GIRK2 mRNA, intensity of the signals and size of the positive areas were similar in both wild-type and mutant mice at P7 (Fig. 2A and C). However, the signal was drastically reduced in adult mutant animals (Fig. 2G).

The number of neurons was significantly decreased in pontine nuclei of weaver mutant mice

To reveal the reason for the significant reduction of *GIRK2* expression in the pontine nuclei of weaver mutants, distribution of neurons in the nuclei was examined in pyronin–methylgreen-stained sections (Fig. 2). A clear boundary was observed between densely stained nuclei and surrounding less stained regions (data not shown). This area contained two groups of cells: one with large cell bodies stained strongly by pyronin (red) and the other with small cell bodies stained strongly by methylgreen (green). The large cells are considered to be projection neurons and the small cells are interneurons and glial cells (Ruigrok & Cella, 1995). GIRK2 mRNA hybridization signals were found mostly in the large cell bodies, suggesting the expression of the gene in projection neurons (Fig. 2B, D and F).

To analyse the degenerating events in the pontine nuclei, we traced the boundaries of the nuclei and counted the number of large cells in every two sections cut at 20 μm thickness. The thickness was set to avoid double counting of the neurons. In wild-type mice, the number of large cells peaked at P9 and then decreased during the later developmental stages (Fig. 3A). The decrement in the late stage might be related to neuronal death in the nuclei, possibly caused by failing to make correct connections with afferents or target cells. Until P7, the total numbers of large cells were similar in both the wild-type and weaver mutant mice. The number, however, decreased to half of the wild type at P9 and to one third at P18 in weaver mutants. Although no changes were detected in the total number of large cells at P7, the distribution of the cells in weaver mutants showed a clear difference from that in wild-type mice (Fig. 3B). At this stage, the number of cells on each slice was higher in the middle region of wild-type nuclei. On the other hand, the number of neurons in weaver mutant mice was decreased strongly in the middle region to shift the peak of neuronal distribution to the rostral side of the nuclei. In the later stages, the number was reduced throughout the whole pontine nuclei.

The changes in 3D structure reflected severe degeneration of the pontine nuclei in weaver mutant mice

The 3D structures of the nuclei were reconstructed based on the shape of boundaries on sections (Fig. 4). At P7 the total volume of the pontine nuclei, estimated from the sum of area size in sections, was

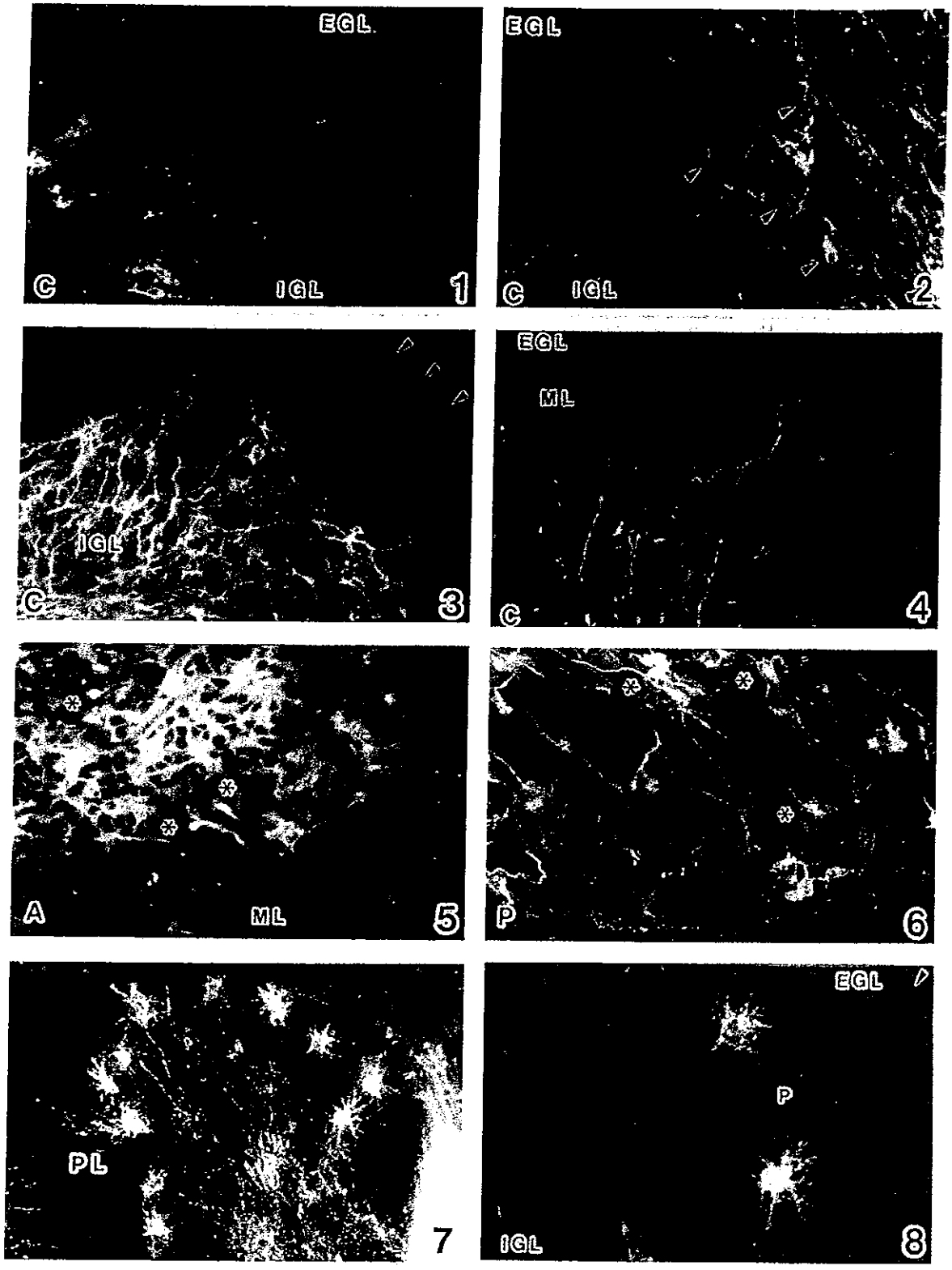

FIG. 5. DiI staining patterns of mossy fibre terminals in the wild type during development. After labelling of mossy fibres at each age in wild-type mice, the vermal part of the cerebellum was sagittally dissected at 200 μm thickness. (1) Central lobe, P1; (2) central lobe, P5, arrowheads indicate stained granule cells; (3) central lobe, P7, arrowheads indicate the surface of the cortex; (4) central lobe, P9; (5 and 6) anterior and posterior lobe, respectively, P14, asterisks indicate mossy fibre terminals; (7 and 8) overall distribution pattern of transiently stained Purkinje cells at P5 in a lobule and its enlarged view (P indicates stained Purkinje cells in panel 8); arrowhead indicates the surface of the lobule. EGL, external granular layer; IGL, internal granular layer; ML, molecular layer; PL, Purkinje cell layer; C, central lobe; A, anterior lobe; P, posterior lobe.

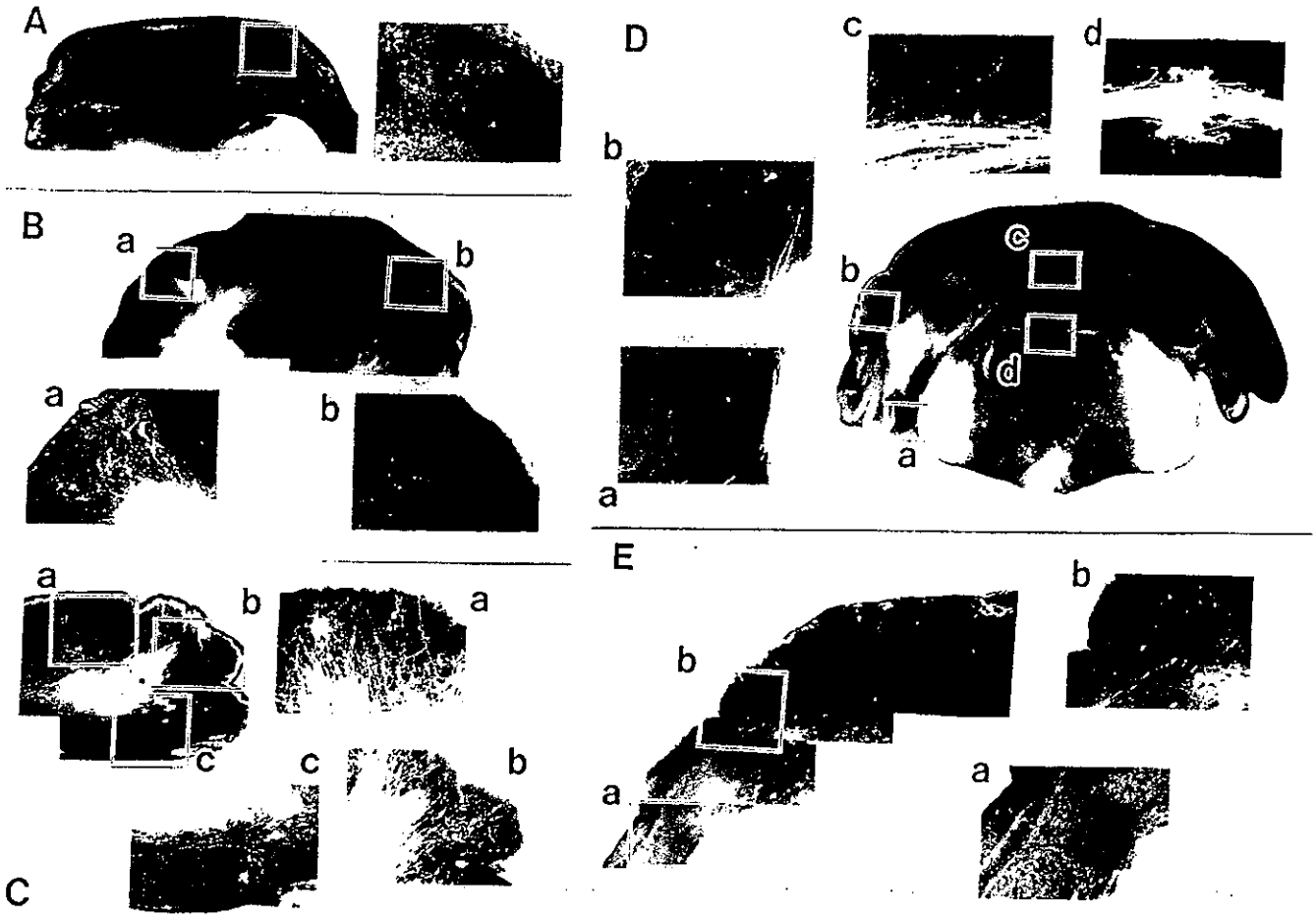

FIG. 6. DiI staining of mossy fibres in weaver mice during development. After labelling of mossy fibres at each age in weaver mutant mice, cerebellar cortices were coronally dissected at 200-μm thickness. (A) P0, (B) P3, (C) P5, (D) P7 and (E) P9. The areas indicated by rectangles are shown in enlarged views.

comparable in wild-type and weaver mice as expected from the similarity in the total number of large neurons (Fig. 4A and B). At P18, however, the volume of the nuclei in weaver mice was reduced to approximately one third of the wild type, whereas the length of the rostrocaudal axis of the nuclei was similar between wild-type and weaver mice (Fig. 4C and D). The reduction in the size in mutants at P18 was well correlated with the reduction in the total number of large-sized neurons, suggesting little change in cell density of the mutant, as was also directly observed in each section. This indicated that neuronal loss was not compensated for by glial cell proliferation in the total volume of the nuclei.

Innervating mossy fibres from the pontine nuclei were eliminated from cerebellar cortex in weaver mutant

DiI, a lipophilic tracer dye, was placed in the dorsal portion of the brachium pontis in order to observe correlation between the degeneration of pontine nuclear neurons and innervation of their axons, pontocerebellar mossy fibres, during development (Figs 5 and 6).

In the vermis of the central lobe of wild-type cerebellum, dotted staining of mossy fibre terminals were sparsely distributed at P1 (Fig. 5, part 1). At P5, a fibrous staining pattern was observed and some granule cells were labelled by DiI in the internal granular layer (Fig. 5, part 2). Densly fibrous staining was observed in the internal granular layer at P7 and even in the molecular layer at P9 (Fig. 5, parts 3 and 4). At P14, the internal granular layer was stained with a mesh-like pattern in the anterior lobe, while densly fibrous staining with bulbous terminals was observed in the posterior lobe, corresponding to the development of glomerular structures at the terminal of mossy fibres and their connections with granule cells.

At P0 and P3, we did not find obvious differences in the mossy fibre innervation pattern between wild-type and weaver mutant mice (Fig. 6A and B). At these stages a fibrous staining pattern was detected in the hemispheres, whereas there were no obvious innervating fibres in the vermis. At P5, however, there were several differences in innervation of mossy fibres between the wild type and the mutant. The density of stained fibres was decreased in the vermis of the mutants, in comparison with that of wild-type animals, whereas a fibrous staining pattern was still observed in the hemispheres (Fig. 6C). Interestingly, some portion of Purkinje cells were stained dispersedly from P3 to P5 in wild-type mice, suggesting transient interaction of pontocerebellar fibres with Purkinje cells during cerebellar development (Fig. 5, parts 7 and 8; Ozaki *et al.*, 1999). In weaver mutant mice, however, it was hard to find staining of Purkinje cells through connection with mossy fibres. By P7, differences in innervation patterns of the fibres between wild-type

